

Remote sensing of the atmosphere with GPS radio occultations



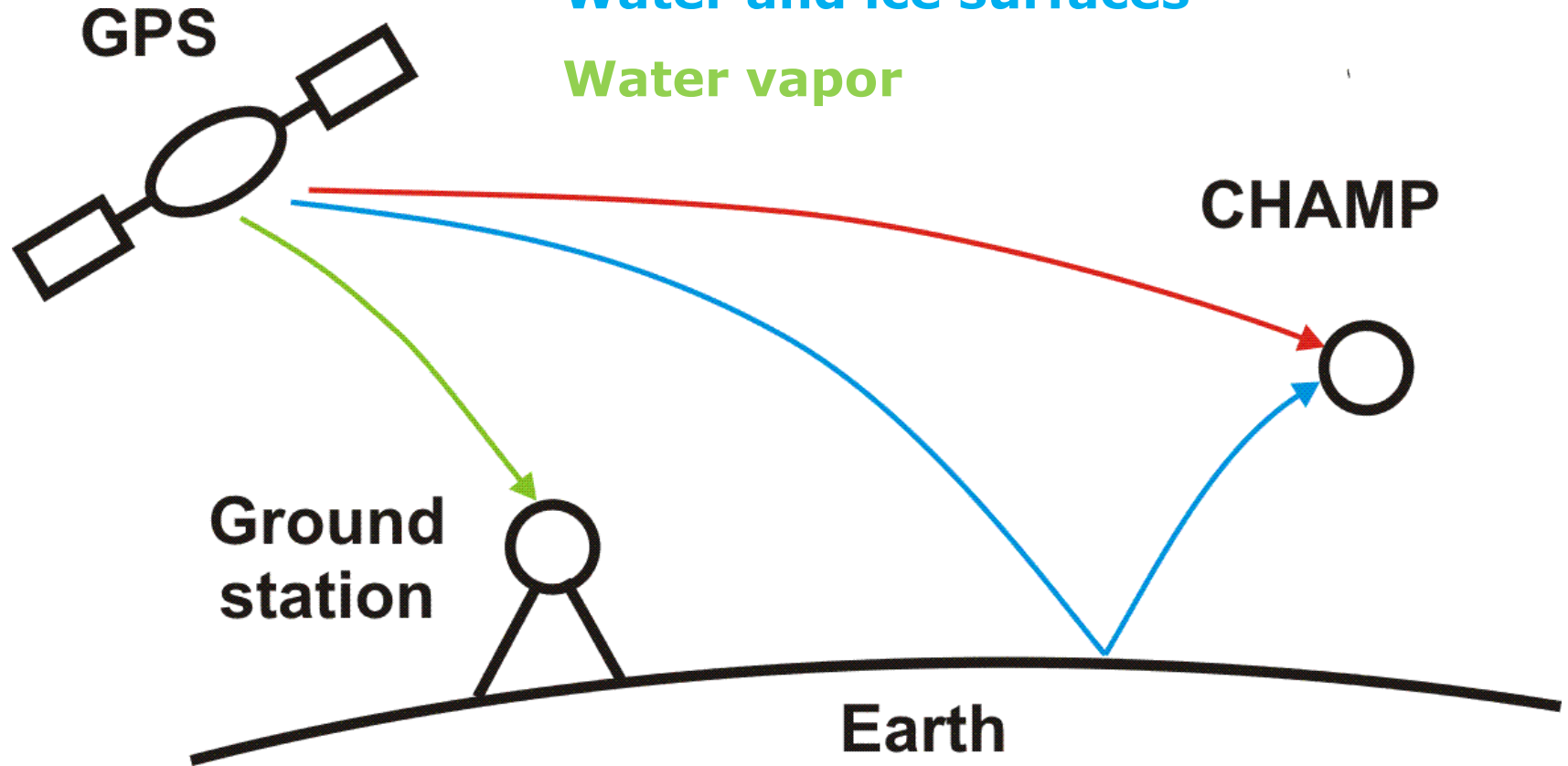
**Torsten Schmidt,
Jens Wickert, Stefan Heise, Georg Beyerle, Florian Zus**
(GFZ German Research Centre for Geosciences, Potsdam)
(Department 1: Geodesy and Remote Sensing)
(Section 1.1: GPS/Galileo Earth Observation)

GNSS-based remote sensing

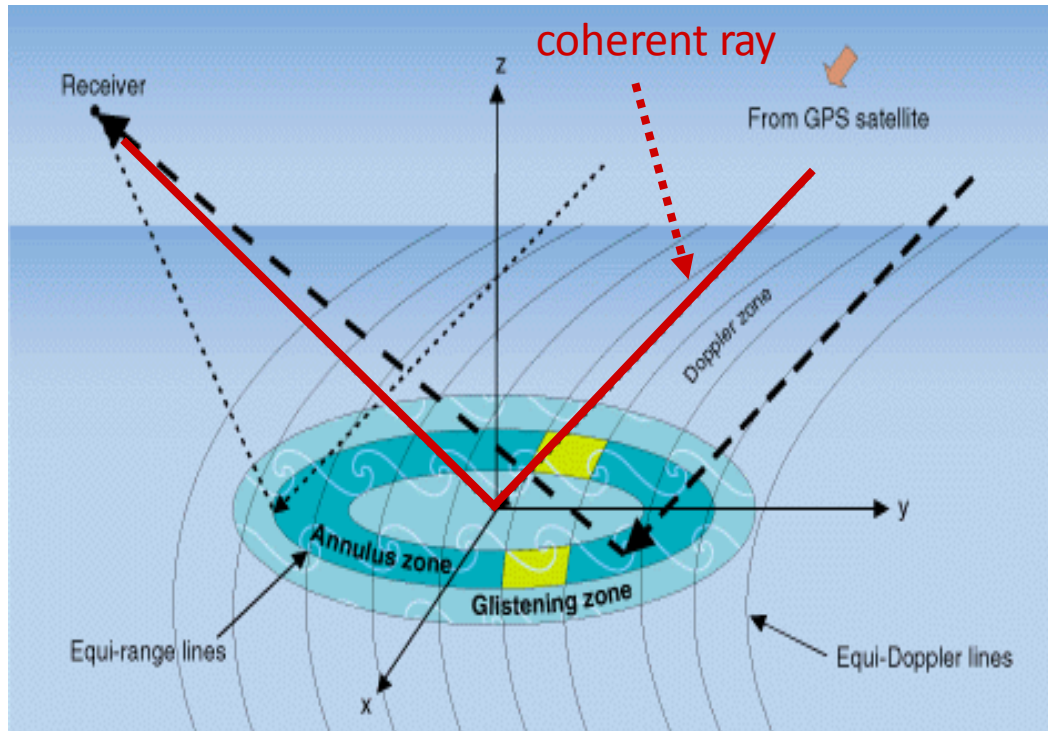
Temperature and water vapor

Water and ice surfaces

Water vapor



GPS reflectometry

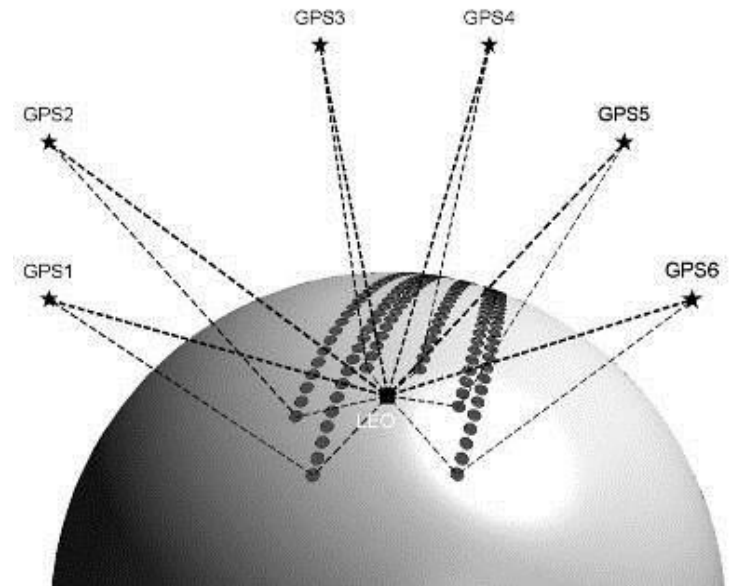


coherent reflection: Interference pattern from **inphase** and **quad-phase correlation sums**

gives information about altimetric heights

incoherent reflection:
Code / Doppler correlation function

gives information about wave heights, wind velocity and direction, absolute heights



(by courtesy of Georg Beyerle, GFZ)

Radio occultation basics

Radio occultation (RO) measurements have been used to study the atmospheres from Mars and Venus since the 1960's.

Its an **active technique**: observe how the paths of radio signals are bent by refractive index gradients in the atmosphere.

The use of RO measurements in the Earth's atmosphere was possible with the **GPS constellation** that provide a suitable source of radio signals.

The proof-of-concept was the NASA **GPS/MET experiment** (1995-1997) that demonstrated the derivation of temperature information.

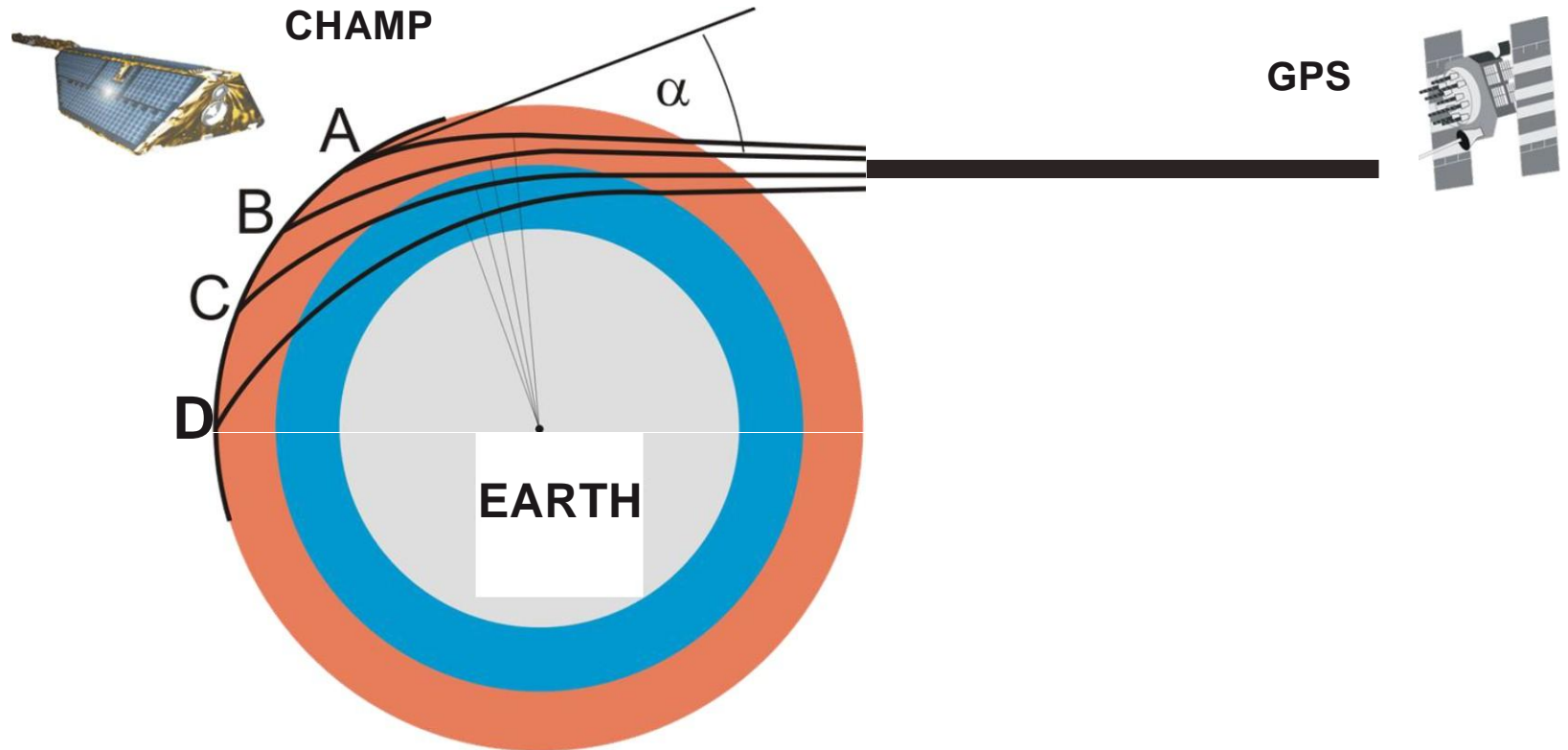
Radio occultation basics

The GPS system is primarily a tool for positioning and navigation. The satellites emit radio signals at **two frequencies L1=1.57 GHz and L2=1.22 GHz** (about 20 cm wavelength).

The GPS signal is influenced by the ionosphere and neutral atmosphere because the refractive index is not constant and the path is bent due to the refractive index gradients in the atmosphere.

GPS RO is based on **analysing the bending** caused by the atmosphere along the ray paths between a GPS satellite and a receiver on-board a low-earth-orbiting (LEO) satellite.

RO measuring principle



RO processing

GPS receivers do not measure bending angle directly!

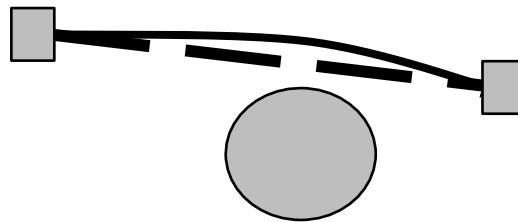
The GPS receiver on the LEO satellite measures a time series of phase-delays $f(i-1)$, $f(i)$, $f(i+1)$,... at the two GPS frequencies:

$$L1 = 1.57542 \text{ GHz}$$

$$L2 = 1.22760 \text{ GHz}$$

The phase delays are “**calibrated**” to remove special and general relativistic effects and to remove the GPS and LEO clock errors (“**Differencing**”, see Hajj et al. (2002), JASTP, **64**, 451 – 469).

Calculate **Excess phase delays**: remove straight line path delay, $Df(i)$.



A time series of Doppler shifts at L1 and L2 are calculated by differentiating the **excess phase delays** with respect to time.

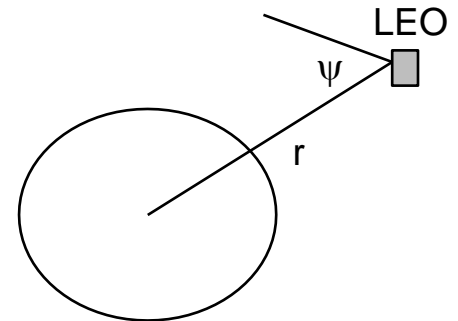
RO processing

The ray bending caused by gradients in the atmosphere and ionosphere modify the L1 and L2 Doppler values, but **deriving the bending angles, α , from the Doppler values is an ill-posed problem.**

The problem made well posed by assuming the impact parameter, given by **(spherical symmetry)**

$$a = nr \sin\psi$$

has the same value at both the satellites.



Given accurate position and velocity estimates for the satellites, and making the impact parameter assumption, the bending angle, α , and impact parameter value can be derived simultaneously from the Doppler.

The ionospheric correction

We have to isolate the atmospheric component of the bending angle. **The ionosphere is dispersive** and so we can take a linear combination of the L1 and L2 bending angles to obtain the “corrected” bending angle. See *Vorob'ev and Krasil'nikov, (1994), Phys. Atmos. Ocean, 29, 602-609.*

$$\alpha(a) = c\alpha_{L1}(a) - (c - 1)\alpha_{L2}(a)$$

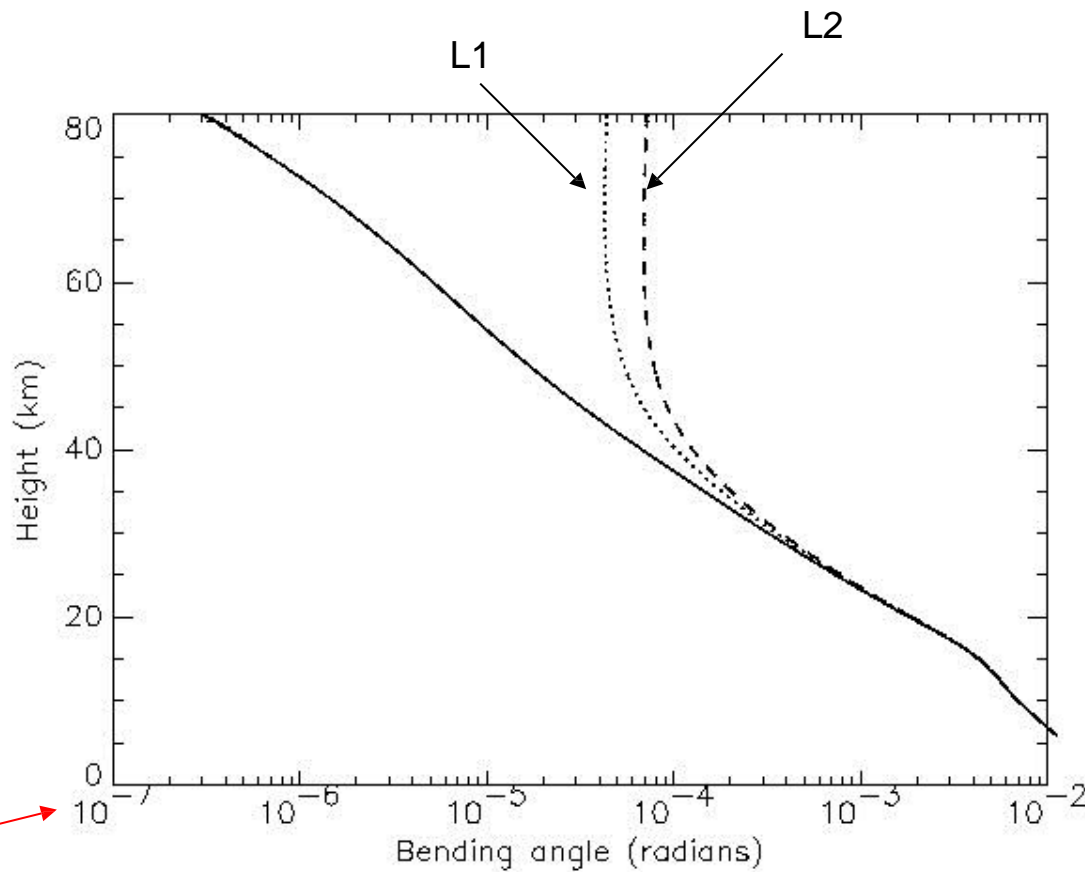
“Corrected” bending angles

Constant given in terms of the L1 and L2 frequencies.

$$c = \frac{f_{L1}^2}{(f_{L1}^2 - f_{L2}^2)}$$

How good is the correction?

The ionospheric correction



The "correction" is very big!

Deriving refractive index profiles

Assuming spherical symmetry the **ionospheric corrected** bending angle can be written as:

$$\alpha(a) = -2a \int_a^{\infty} \frac{d \ln n / dx}{\sqrt{x^2 - a^2}} dx$$

Corrected Bending angle
as a function of impact parameter

Convenient variable ($x=nr$)
(refractive index * radius)

We can use an Abel transform to derive a refractive index profile

$$n(x) = \exp \left(\frac{1}{\pi} \int_a^{\infty} \frac{\alpha(a)}{\sqrt{a^2 - x^2}} da \right)$$

Note the upper-limit of the integral! A priori needed.

Temperature and pressure profiles

“Classical retrieval”

The refractive index (or refractivity) is related to the pressure, temperature and water vapour pressure.

refractivity →

$$N = 10^6 (n - 1)$$
$$= \frac{c_1 P}{T} + \frac{c_2 P_w}{T^2}$$

This is two term expression is probably the simplest formulation for refractivity, but it is widely used in GPS RO.

If the water vapour is negligible, the 2nd term = 0, and the refractivity is proportional to the density:

$$N \approx \frac{c_1 P}{T} = c_1 R \rho$$

So we have derived a vertical profile of density!

Temperature and pressure profiles

“Classical retrieval”

We can derive the pressure by integrating the **hydrostatic equation**:

$$P(z) = P(z_u) - \frac{1}{c_1 R} \int_z^{z_u} N(z) g(z) dz$$

a priori

The temperature profile can then be derived with the **ideal gas law**:

$$T(z) = c_1 \frac{P(z)}{N(z)}$$

GPS/MET experiment (1996): Groups from JPL and UCAR demonstrated that the retrievals agreed with co-located analyses and radiosondes to within 1 K between ~5-25 km.

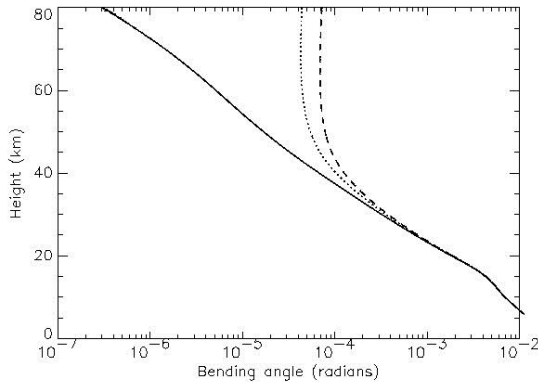
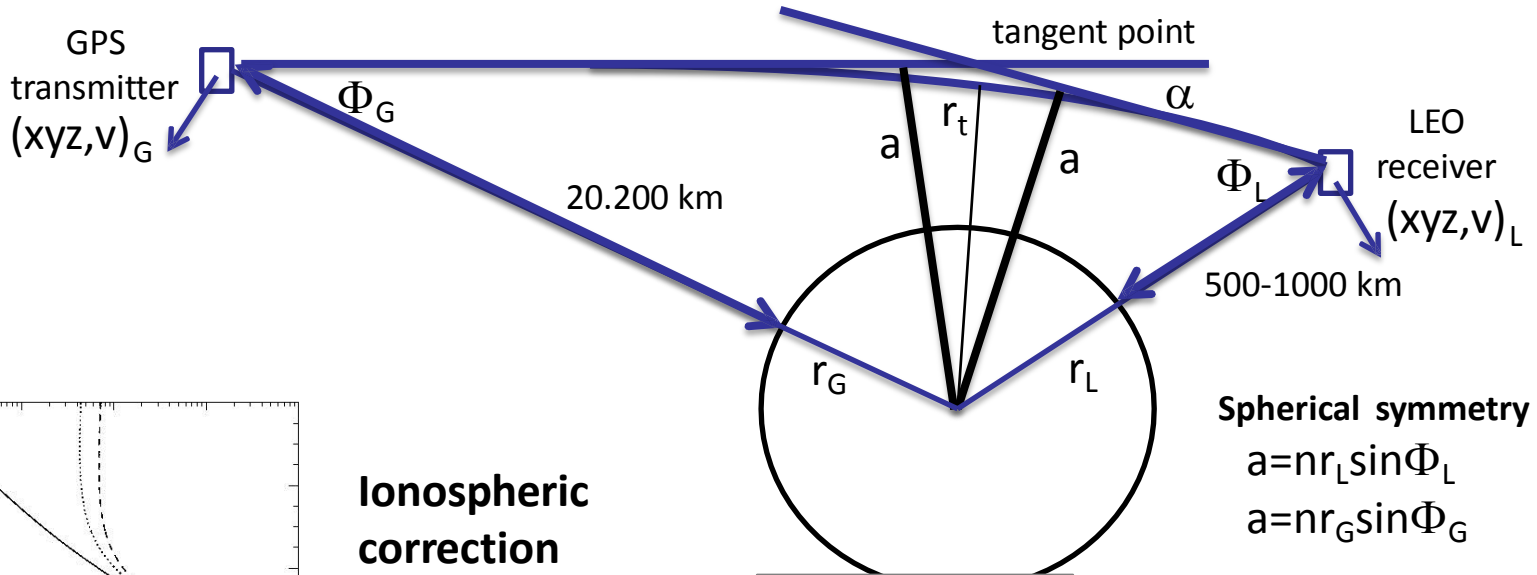
See Rocken et al., 1997, JGR, 102, D25, 29849-29866.

RO characteristics

- Good vertical resolution. Around 70% of the bending occurs over a ~ 450 km section of ray-path, centred on the tangent point (*point closest to surface*) – **it has a broad horizontal weighting function!**
- All weather capability: not affected by cloud or rain.
- The bending is ~ 1 -2 degree at the surface, falling exponentially with height. The scale-height of the decay is approximately the density scale-height.
- A profile of bending angles from ~ 60 km tangent height to the surface takes about 2 minutes. Tangent point drifts in the horizontal by ~ 150 km during the measurement.

Radio occultation processing steps

a = distance of closest approach for the straight line path.



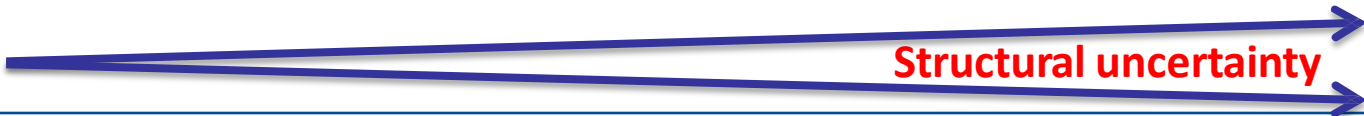
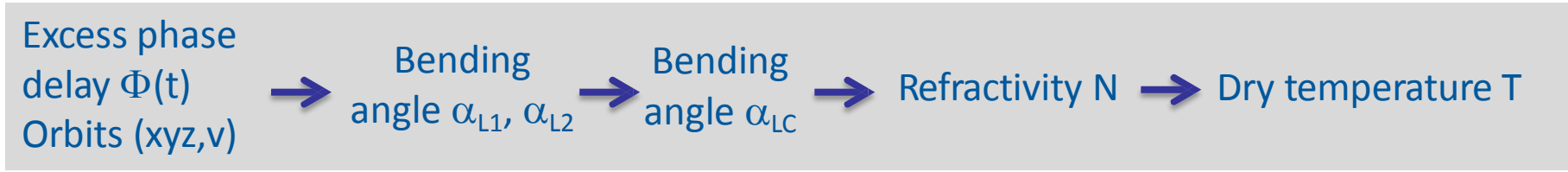
Ionospheric correction
a priori $\alpha > x$ km
“statistical optimization”

$$\ln n(r) = \frac{1}{\pi} \int_a^\infty da' \frac{\alpha(a')}{\sqrt{a'^2 - a^2}}$$

Abel transform

Spherical symmetry
 $a = nr_L \sin \Phi_L$
 $a = nr_G \sin \Phi_G$

neglect p_w hydrostatic app. a priori pressure

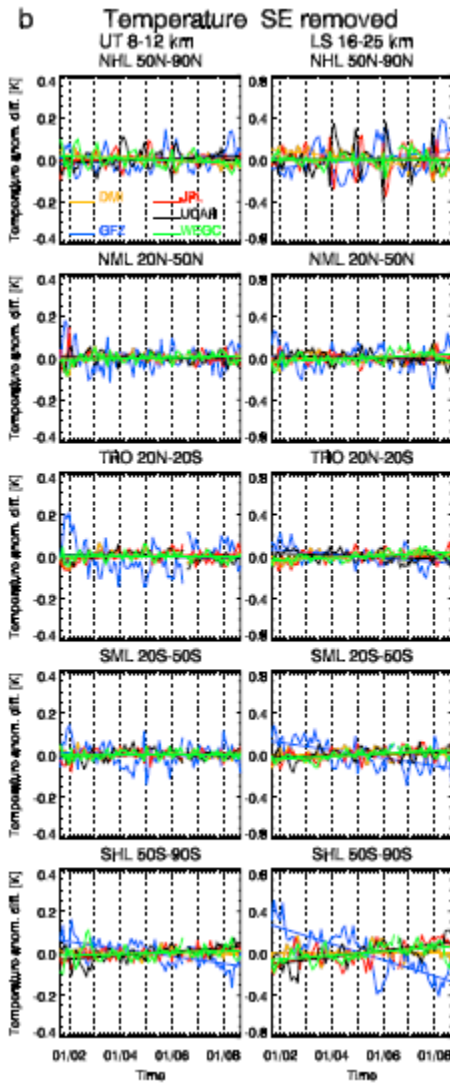


RO center inter-comparison

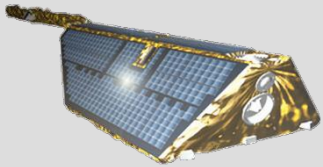
Steiner et al., Quantification of structural uncertainty in climate data records from GPS radio occultation, Atmos. Chem. Phys., 13, 1469–1484, www.atmos-chem-phys.net/13/1469/2013/ doi:10.5194/acp-13-1469-2013, 2013.

DMI Copenhagen, EUM Darmstadt, GFZ Potsdam, JPL Pasadena, UCAR Boulder, and WEGC Graz

“We find that structural uncertainty is lowest in the tropics and mid-latitudes (50°S to 50°N) from 8 km to 25 km for all inspected RO variables. In this region, the structural uncertainty in trends over 7 yr is <0.03 % for bending angle, refractivity, and pressure, <3 m for geopotential height of pressure levels, and <0.05 K for temperature; low enough for detecting a climate change signal within about a decade. Larger structural uncertainty above about 25 km and at high latitudes is attributable to differences in the processing schemes, which undergo continuous improvements. Though current use of RO for reliable climate trend assessment is bound to 50°S to 50°N, our results show that quality, consistency, and reproducibility are favorable in the UTLS for the establishment of a climate benchmark record.”

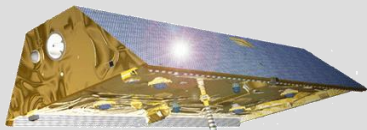


Radio occultation missions



2001 – 2008

CHAMP (GFZ)



since 2006

GRACE (GFZ)



since 2008/10

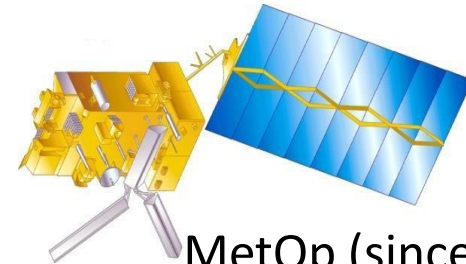
TerraSAR-X/Tandem-X
(GFZ)



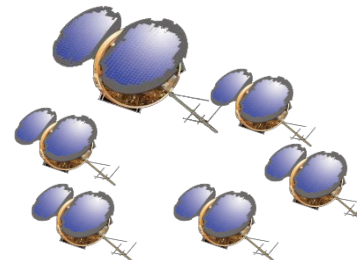
SAC-C

(2001 ... 2011)

GPS/MET
(1995/97)



MetOp (since 2006)

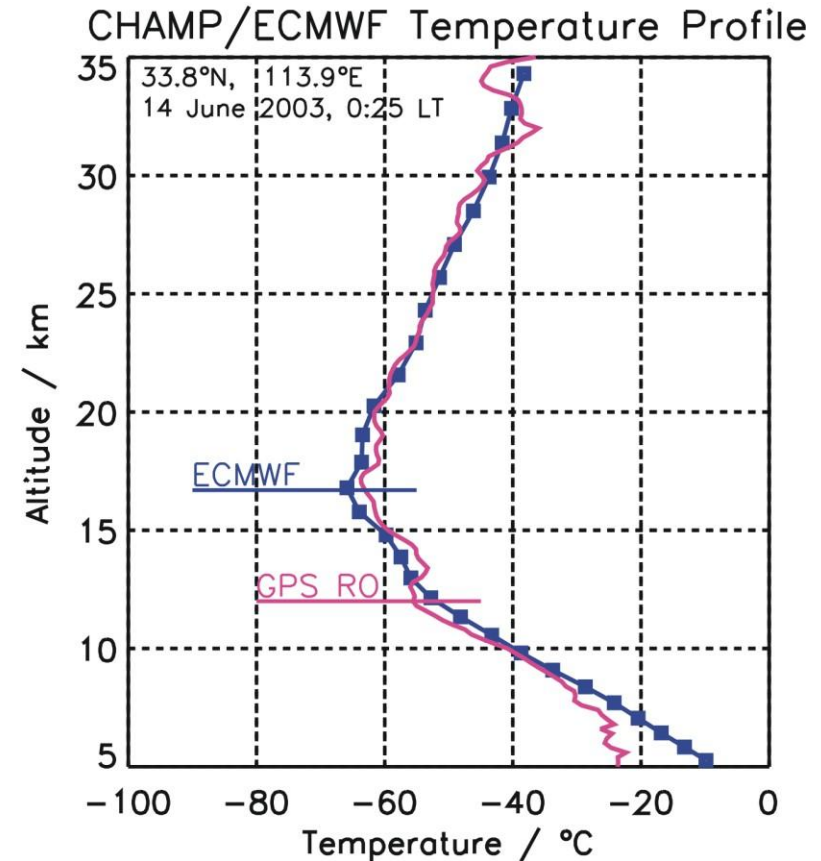
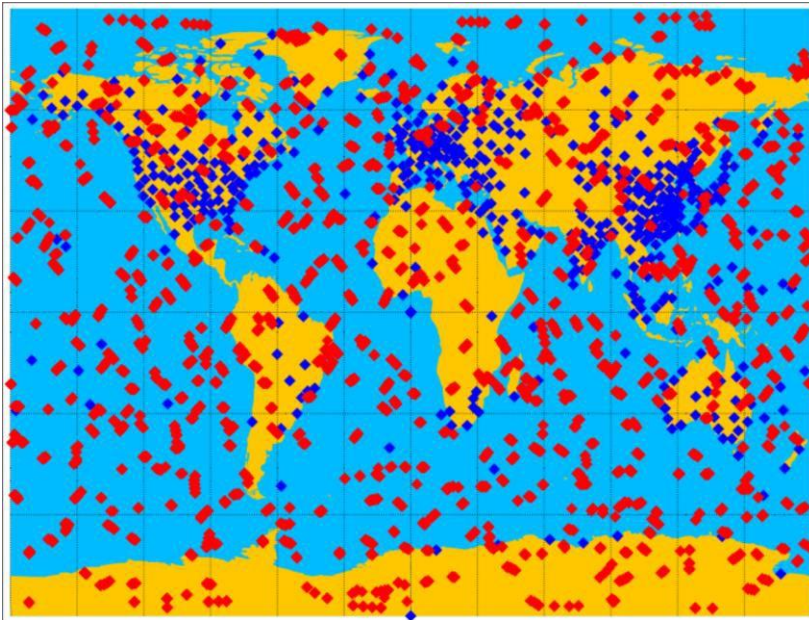


COSMIC/FORMOSAT-3

(since 2006)

Properties of the RO technique

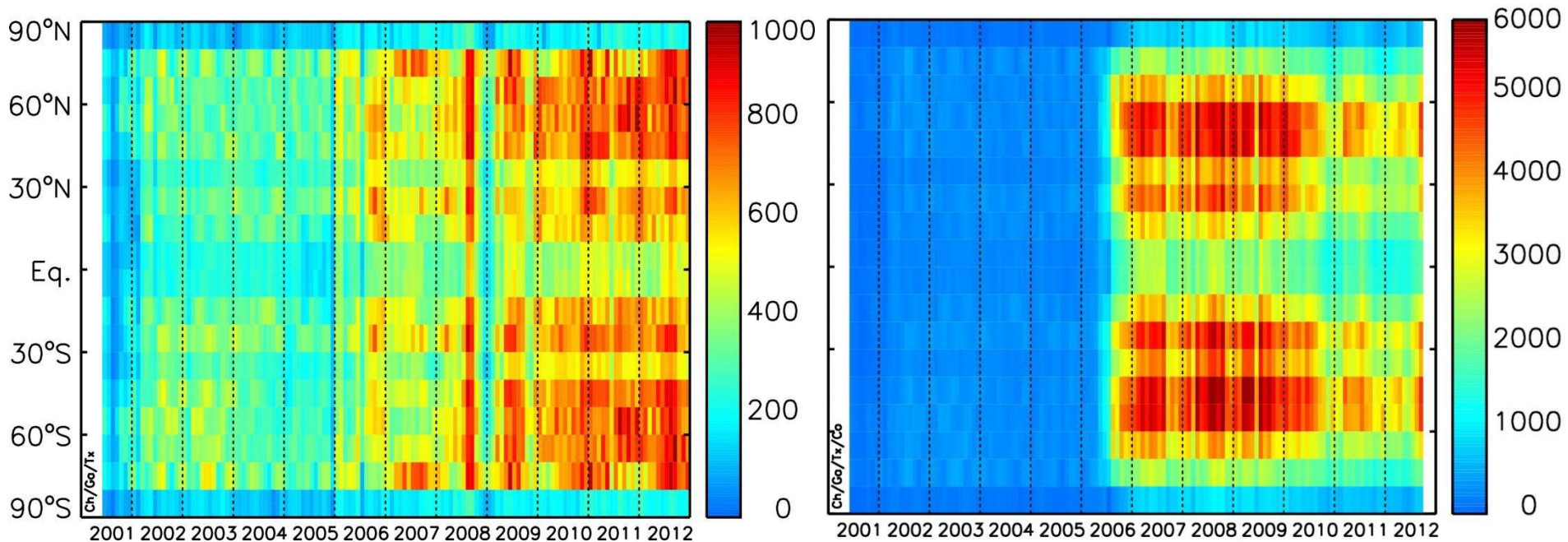
- high vertical resolution
- global coverage
- weather independent
- calibration free
- long-term stable



Data base: >1 decade

GFZ: CHA/GRA/TSX

UCAR: CHA/GRA/TSX/COS



Next

GRACE-FO (2017)
GEROS-ISS (~2016, 10 yrs)

COSMIC-2 (2017)

RO applications

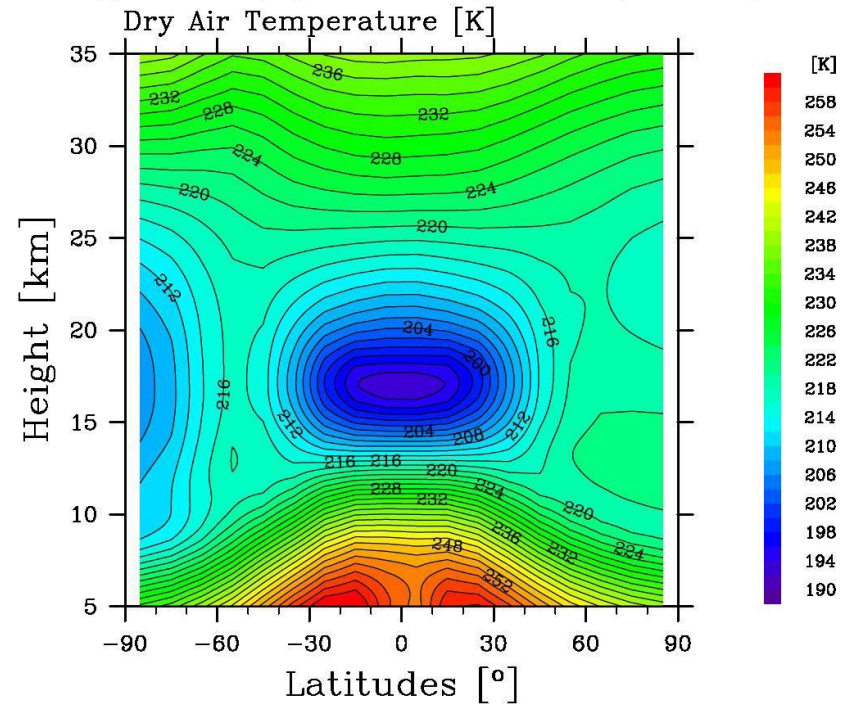
Weather forecast



RO data were used since 2006 by
ECMWF, Met Office, DWD, Meteo France,
NCEP/NOAA, Japanese Weather Service,
Environment Canada, ...

Climate and atmospheric studies

Climatology GPS RO (High Resolution) mean 05/2001–12/2010



(by courtesy of Sara Stege, GFZ)

RO impact on ECMWF

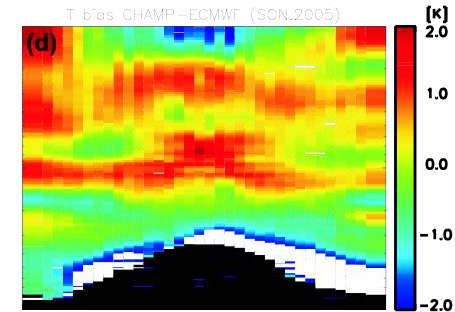
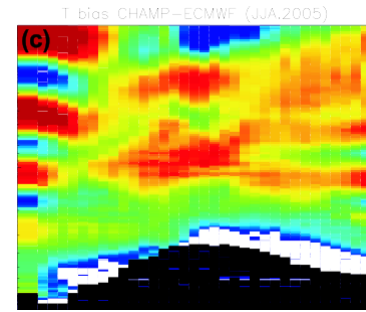
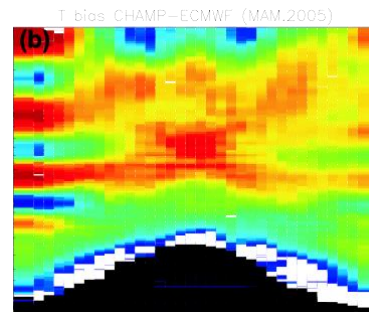
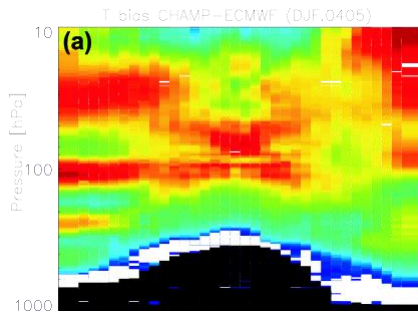
DJF

MAM

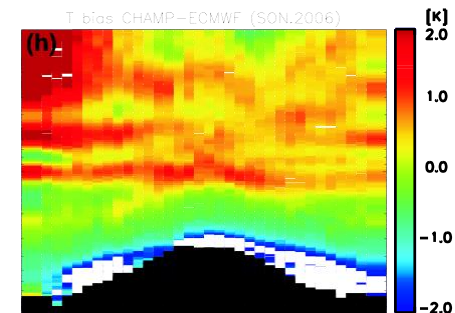
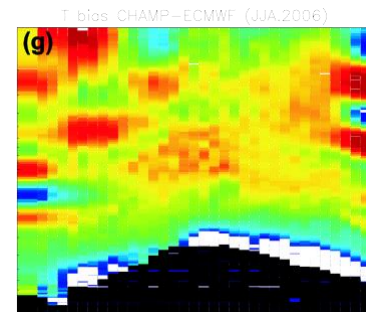
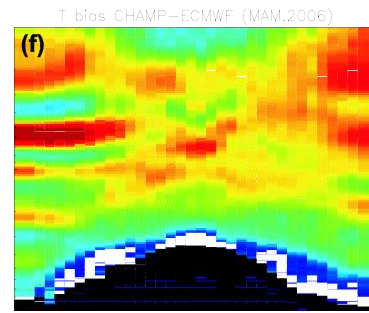
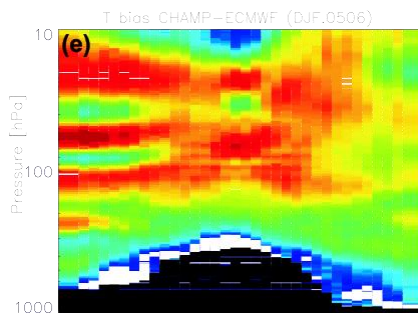
JJA

SON

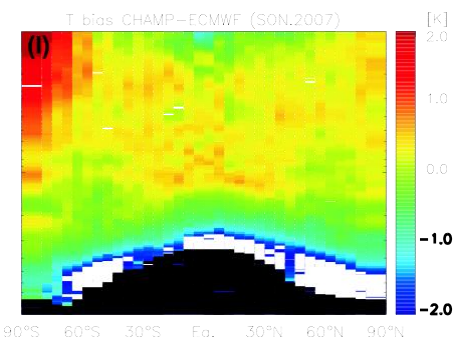
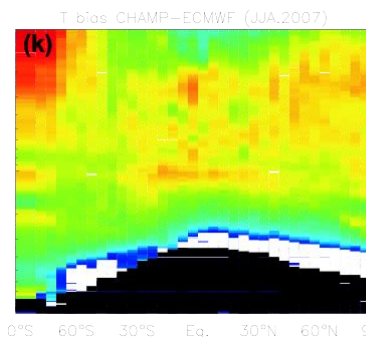
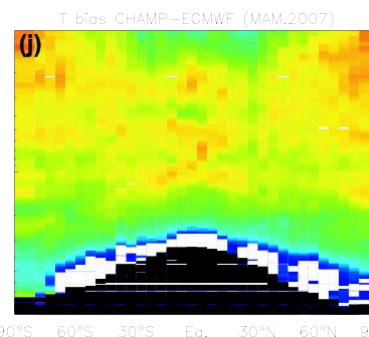
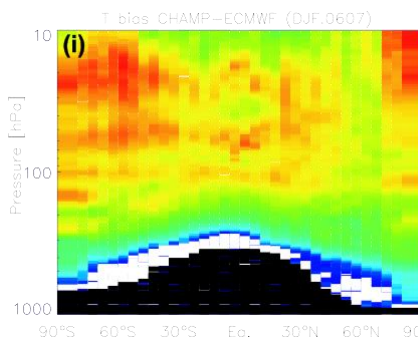
2005



2006



2007



(from Schmidt et al., AG, 2008)

NTR data processing

http://www-app2.gfz-potsdam.de/pb1/GASP/GASP2/CHAMP/RO_EXPERIMENT/index_ro_experiment.html

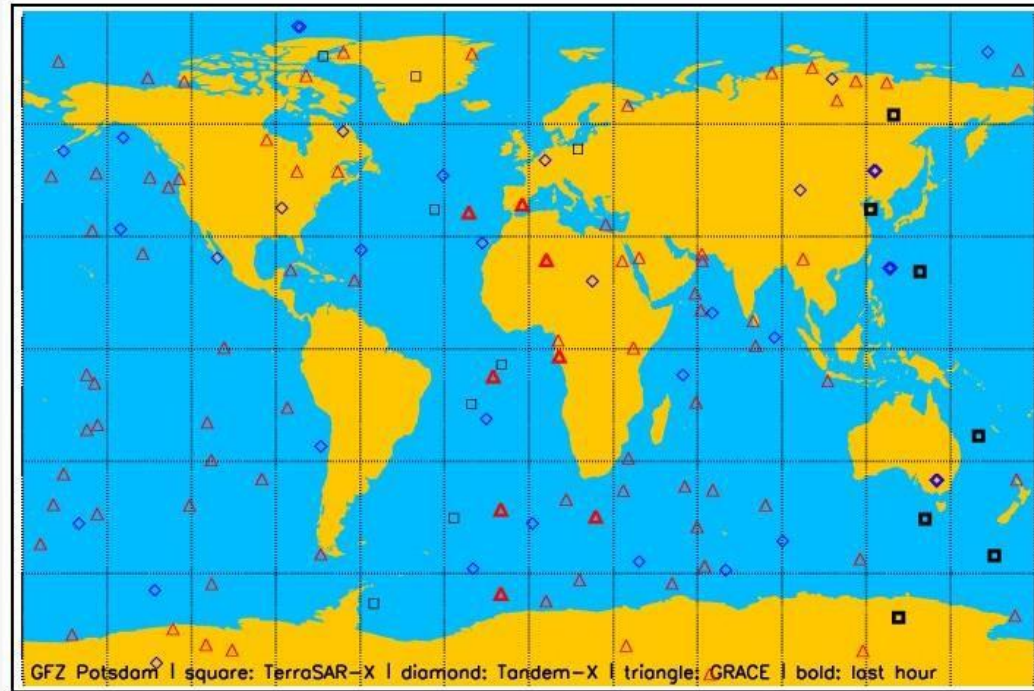
GFZ
POTSDAM

GFZ home

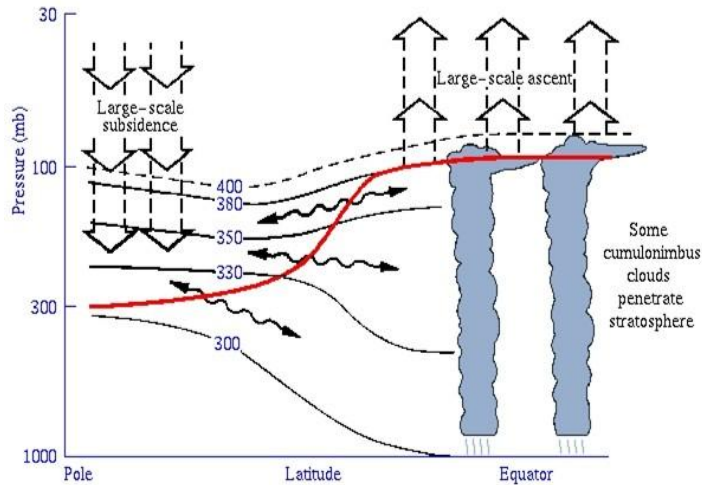
NRT processing

Near-real time radio occultation with TerraSAR-X, Tandem-X and GRACE

2014-09-16 (Day of Year: 259)



Atmospheric studies using RO data



Tropopause height as indicator for climate change

Tropopause dynamics (tropopause inversion layer)

GPS RO:

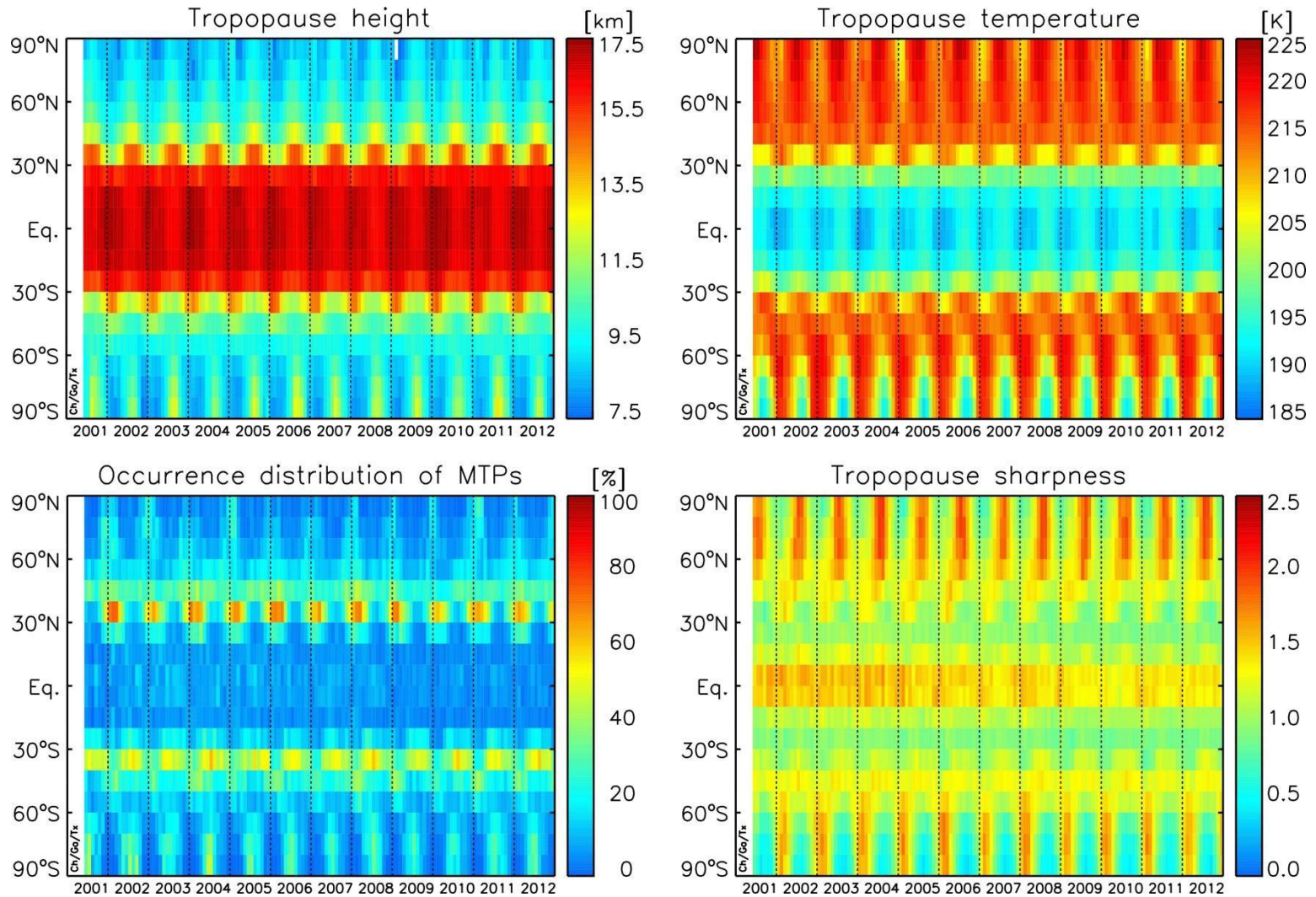
Monitoring tropopause characteristics and UTLS temperature structure

Importance of gravity waves (GW) for the global circulation and structure of the atmosphere

GPS RO:

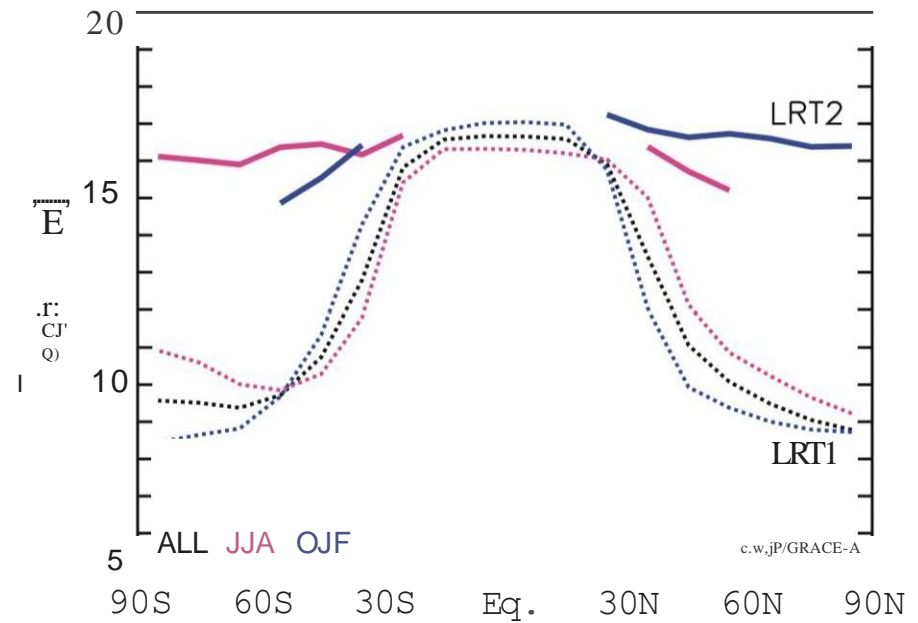
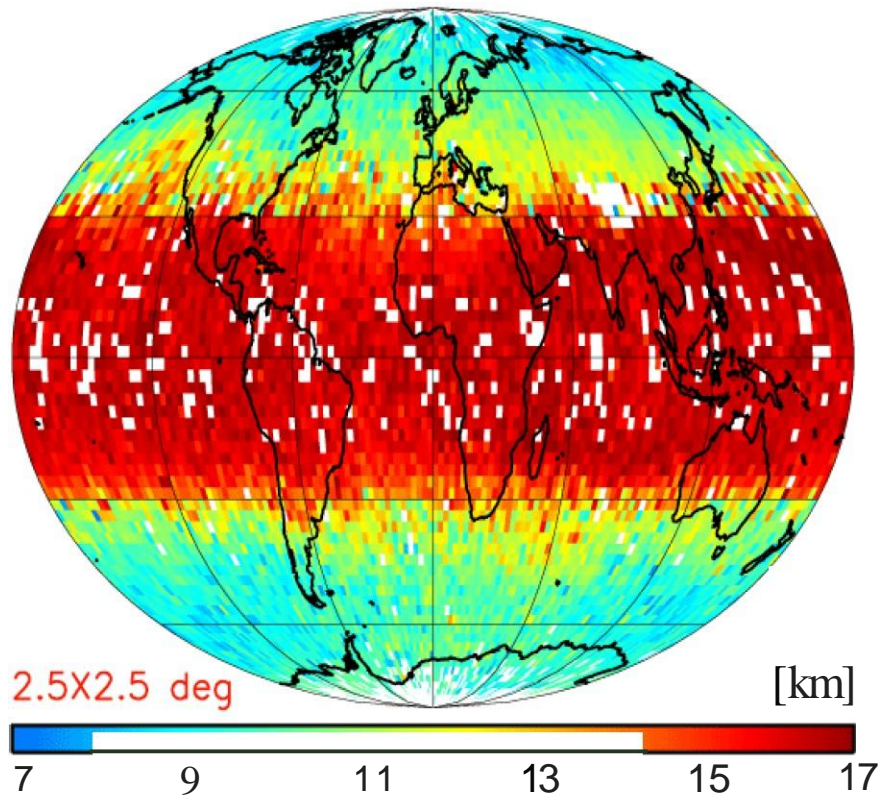
Monitoring the GW activity (source regions)

Tropopause characteristics



(update from Schmidt et al., JGR 2004, ACP 2005, GRL 2006)

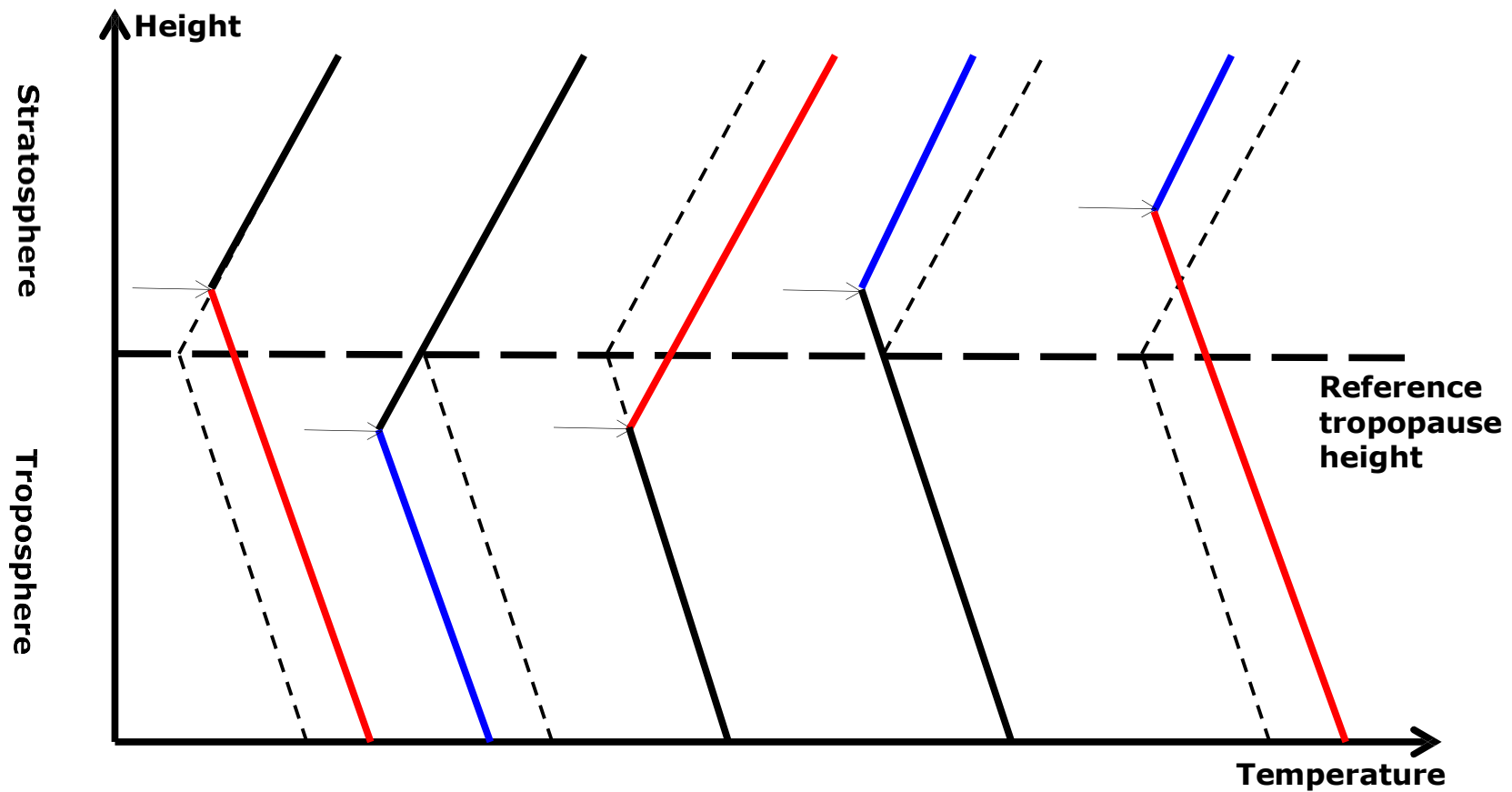
Tropopause height



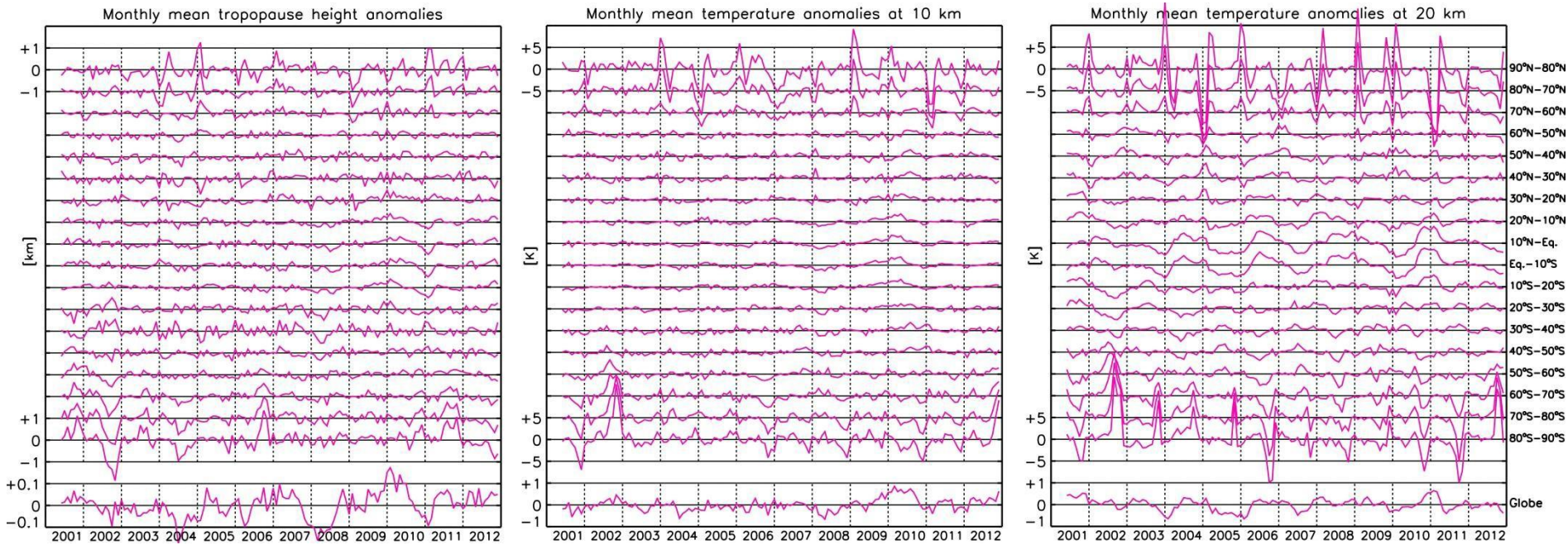
Tropopause and UTLS temperatures

Tropopause forcing mechanisms

Tropospheric/stratospheric **warming** and **cooling**



De-seasonalized monthly means

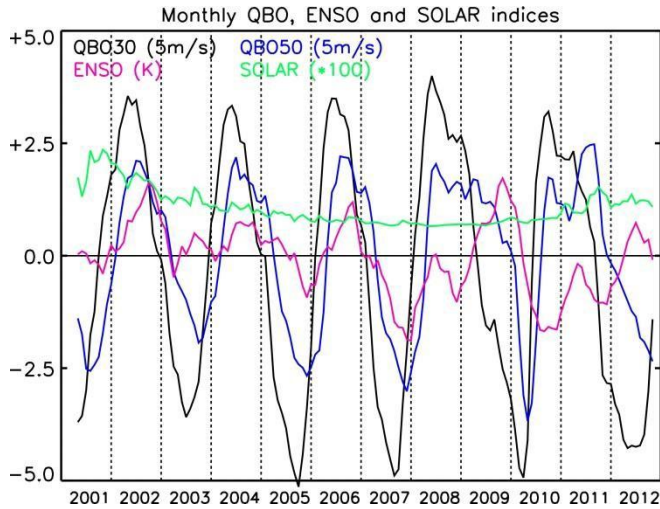


$$\Delta(\phi, z, t) = \Delta + \Delta \cdot t + \Delta_1 \cdot QB(30) t + \Delta_2 \cdot QB(50) t + \Delta \cdot t \quad (1)$$

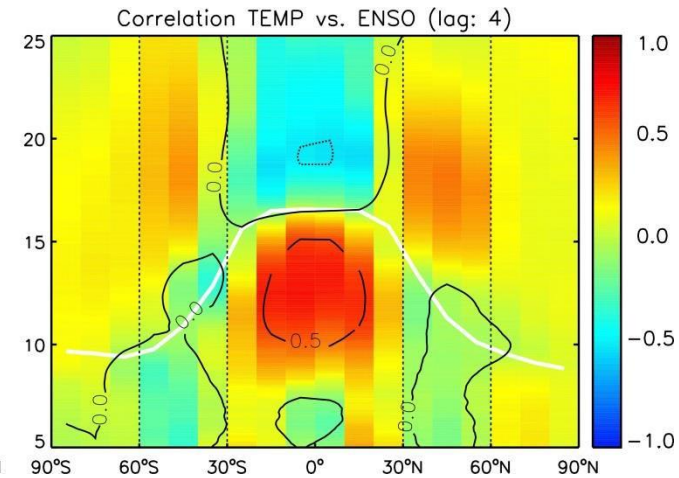
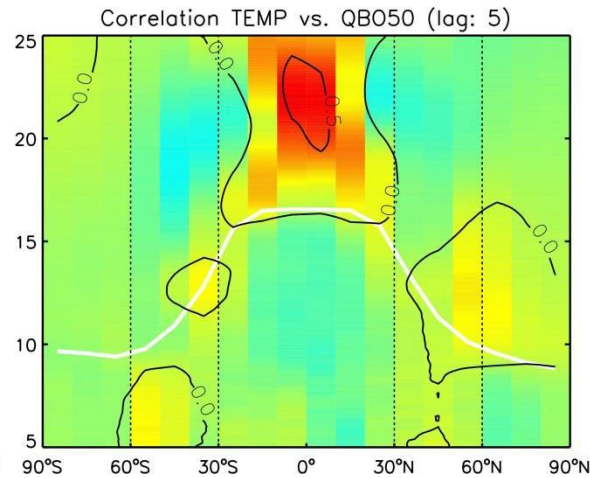
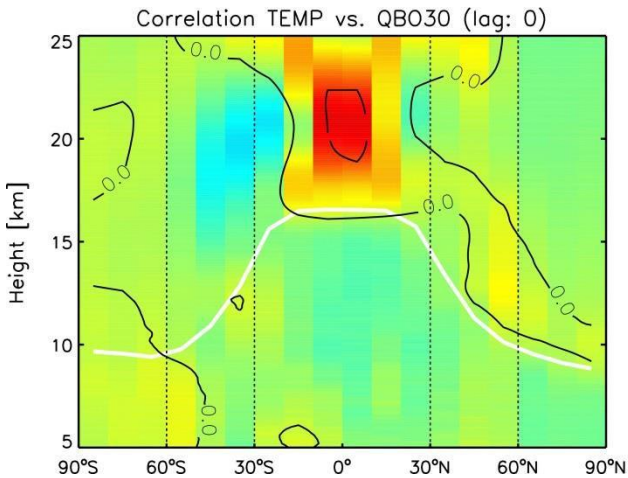
Basis: CHAMP/GRACE/TerraSAR-X (June 2001-December 2012)

(update from Schmidt et al., GRL 2008, ASR 2010)

Correlation: Temp vs. QBO and ENSO

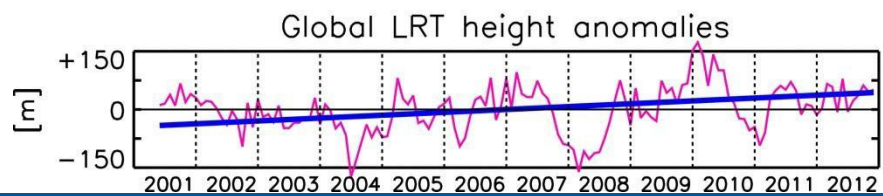
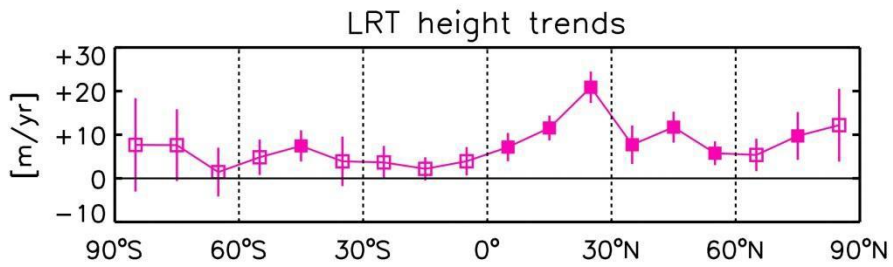
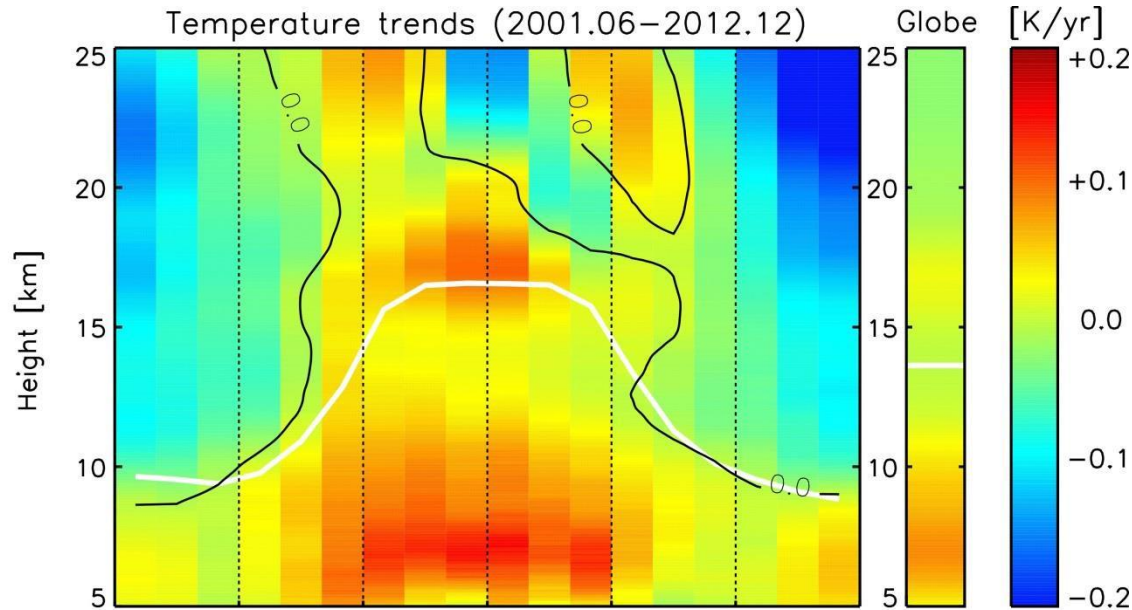


indices from <ftp://ftp.cpc.ncep.noaa.gov/wd52dg/data/indices> (ENSO=NINO3.4)

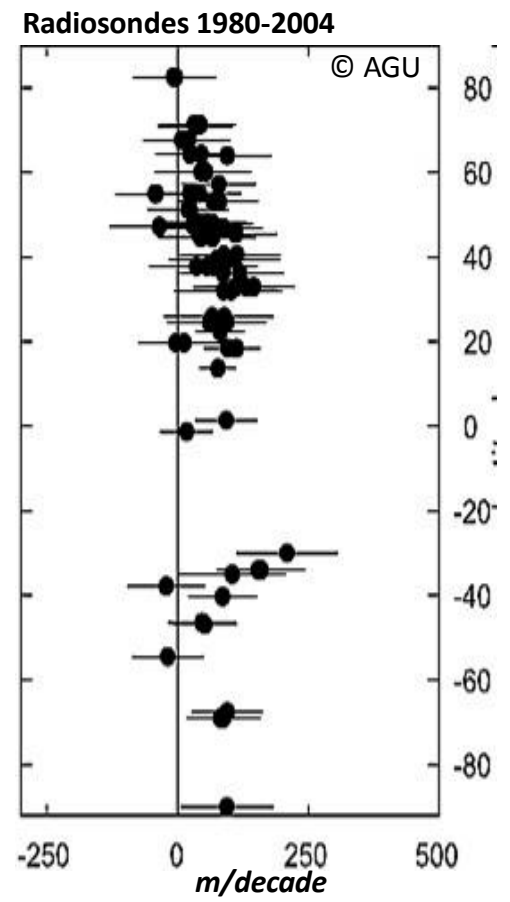


Basis: CHAMP/GRACE/TerraSAR-X (June 2001-December 2012)

Temperature and tropopause height trends



Global
7 ± 1 m/yr

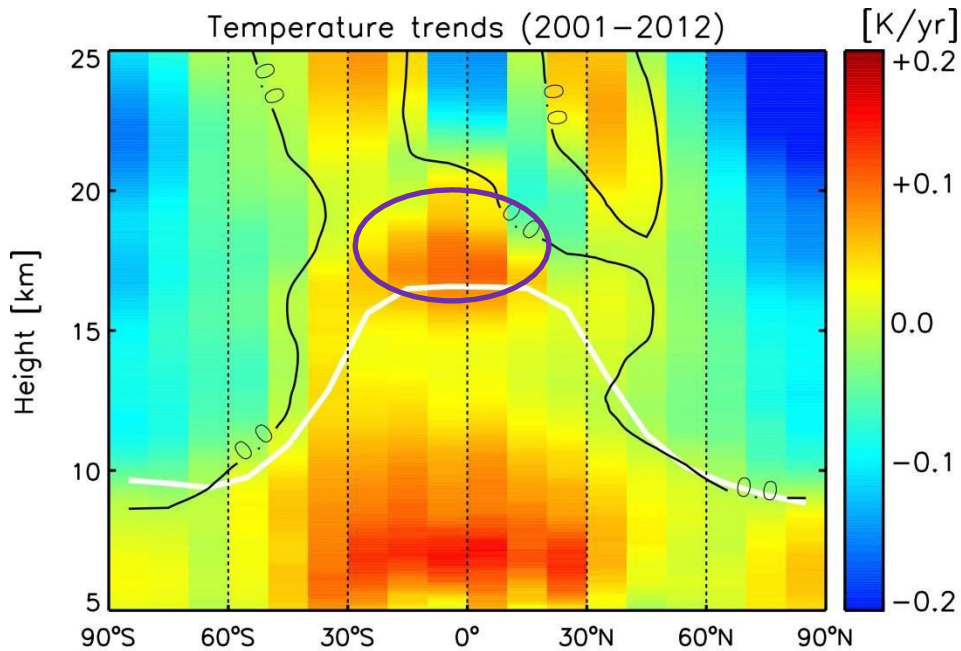


Seidel & Randel, JGR, 2006

Basis: CHAMP/GRACE/TerraSAR-X
June 2001-December 2012

Temperature trends

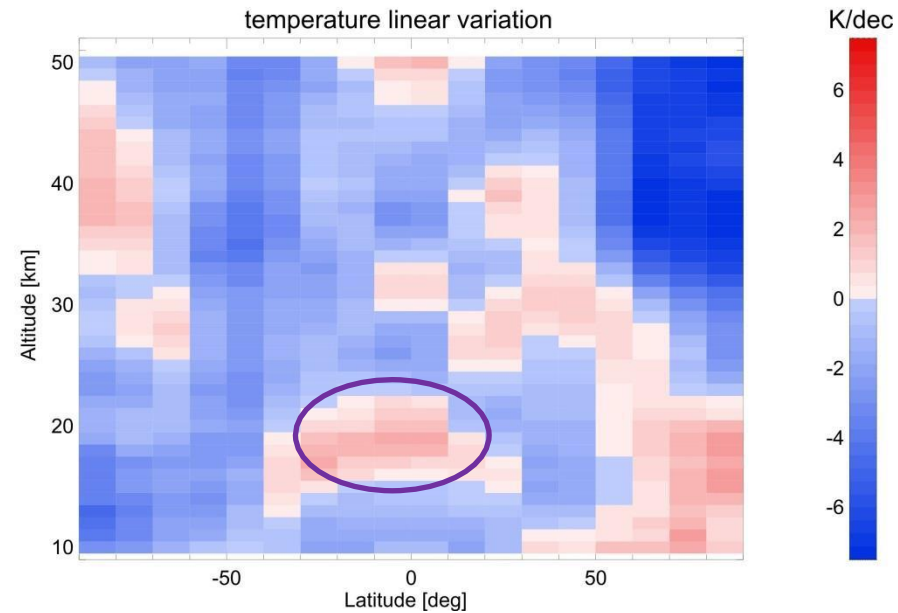
RO



(update from Schmidt et al., ASR, 2010)

MIPAS

2002-2012

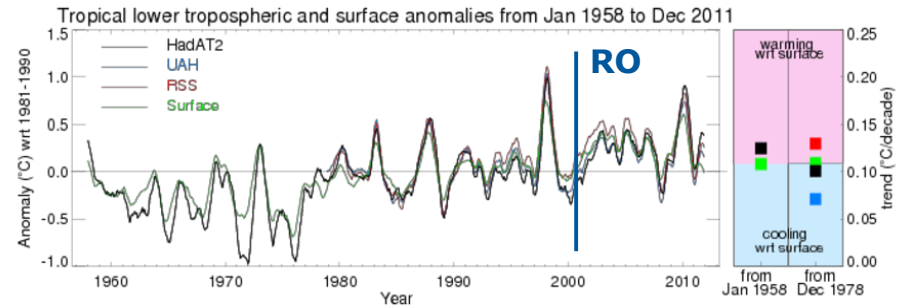
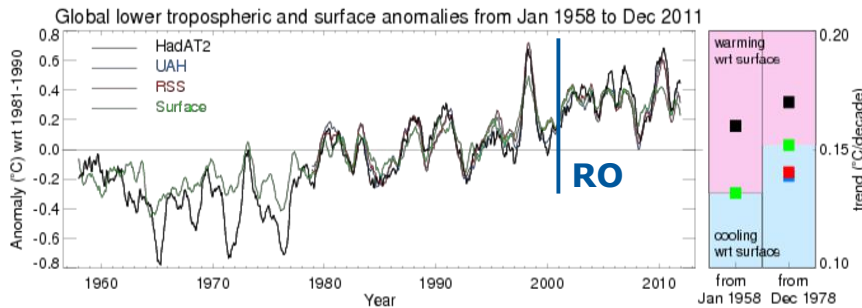
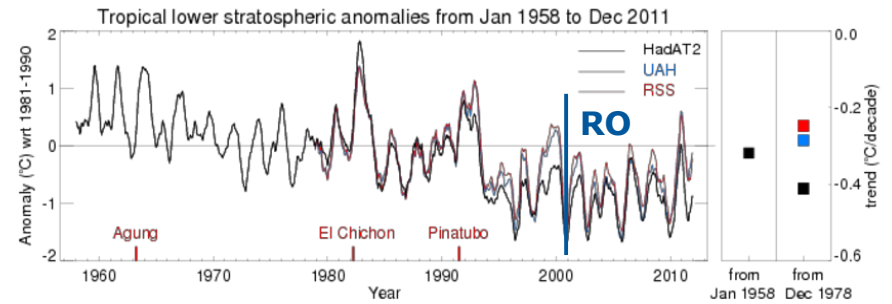
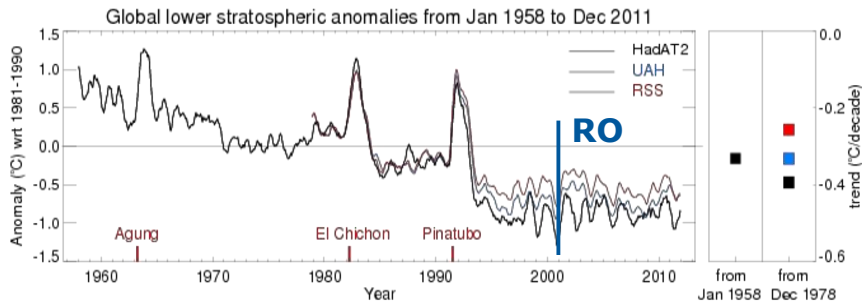


(by courtesy of Ellen Eckert, KIT)

Temperature trends

Long-term data from radiosondes and MSU data

<http://www.metoffice.gov.uk/hadobs/hadat/images.html>



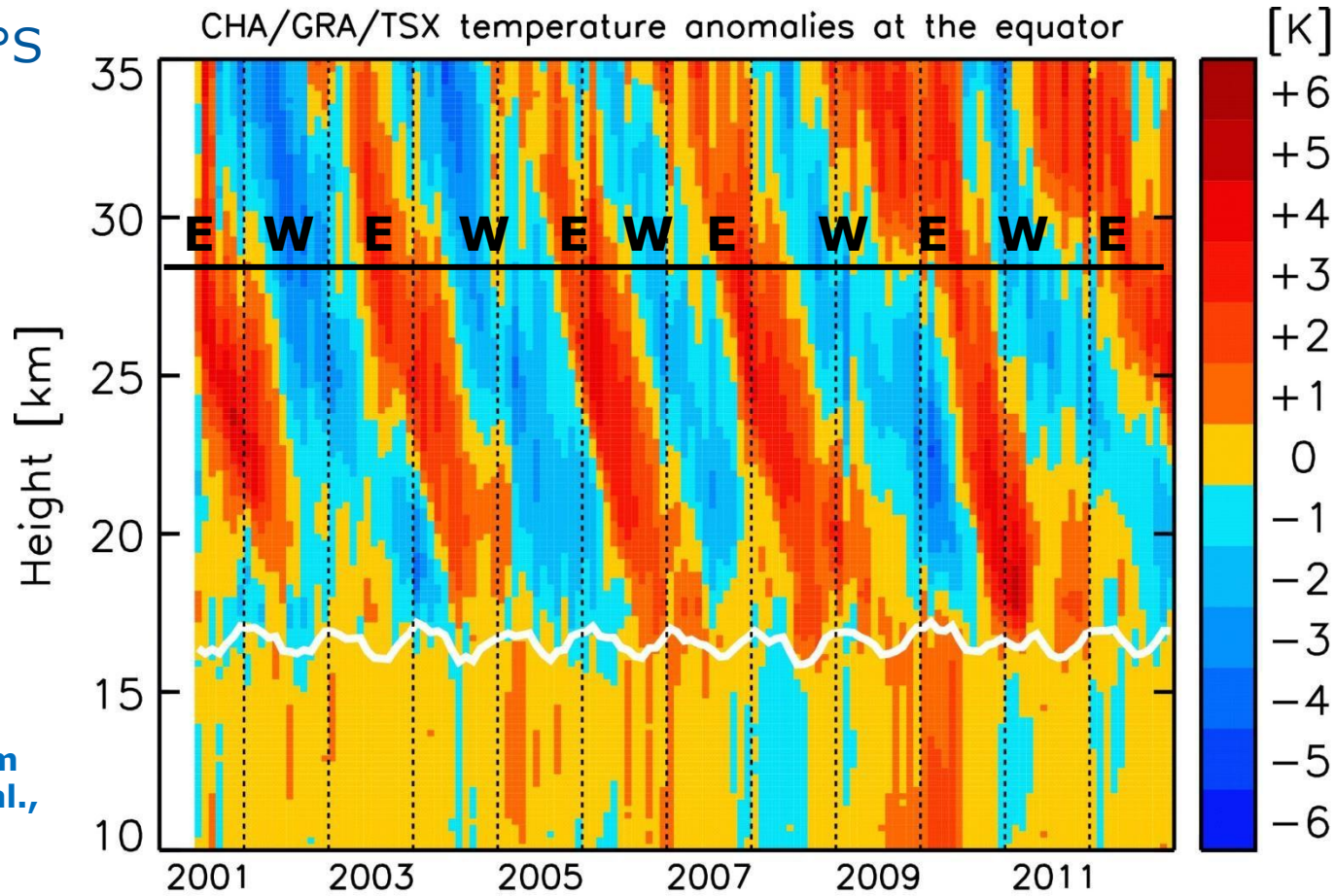
HadAT2 radiosonde data and HadCRUT3 surface data are produced by the Hadley Centre and are available at www.hadobs.org
 UAH MSU satellite data are produced by the University of Alabama in Huntsville and are available at www.nsstc.uah.edu/public/msu courtesy of John Christy and Roy Spencer
 RSS MSU satellite data are produced by Remote Sensing Systems and are available at www.rms.com courtesy of Carl Mears

HadAT2 radiosonde data and HadCRUT3 surface data are produced by the Hadley Centre and are available at www.hadobs.org
 UAH MSU satellite data are produced by the University of Alabama in Huntsville and are available at www.nsstc.uah.edu/public/msu courtesy of John Christy and Roy Spencer
 RSS MSU satellite data are produced by Remote Sensing Systems and are available at www.rms.com courtesy of Carl Mears

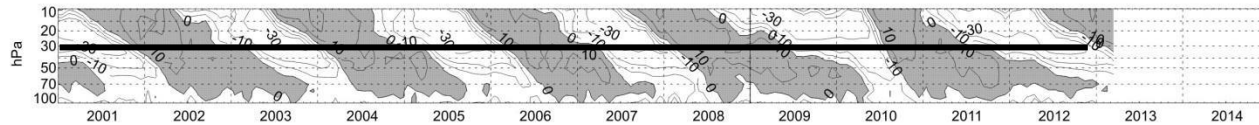
QBO in the RO temperature data

10°N-10°S

CHA/GRA/TSX temperature anomalies at the equator

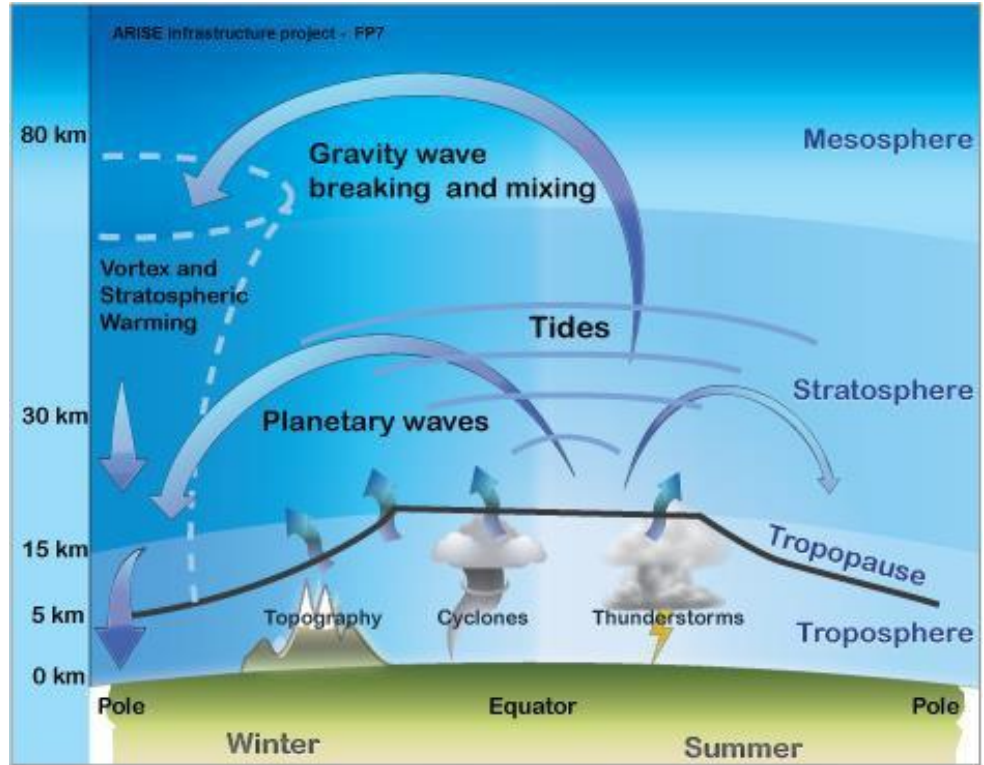
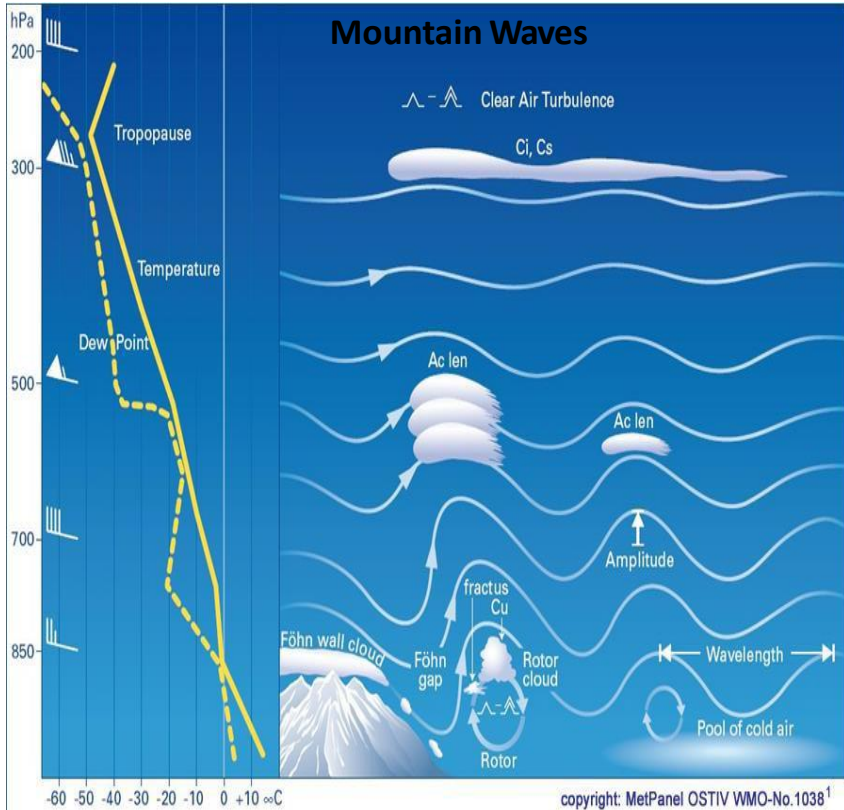


(update from Schmidt et al., ACP 2005)



www.geo.fu-berlin.de/met/ag/strat/produkte/qbo/

Gravity waves



From the ARISE (Atmospheric dynamics Research Infrastructure in Europe) homepage

Gravity wave analysis

Vertical flux of horizontal momentum
(momentum flux)

$$\overline{p(z)} = \rho(z) \cdot \lambda \frac{\lambda_z(z)}{h(z)} \cdot \overline{p(z)}$$

$$\overline{p(z)} = \overline{p(z)} - \overline{p(z)}$$

$$\overline{p(z)} = \frac{\overline{p(z)}}{\overline{p(z)}} \cdot \left(\frac{\overline{p(z)}}{\overline{p(z)}} \right)$$

$$\overline{p(z)} = \frac{1}{\overline{p(z)}} \cdot \overline{p(z)}^2$$

$$\lambda_z(z) \cdot \overline{p(z)}$$

$$\overline{p(z)} \cdot \lambda_h(z) = \rho(z) \cdot \lambda_z(z) \cdot \overline{p(z)}$$

$$\frac{k_h}{k_z} = \overline{N}$$

Fröhlich et al. (2007): $\frac{k_h}{k_z} = 3$
 $\lambda_h(z) = \frac{\lambda_z(z)}{3}$ with $150k \leq \lambda_h \leq 1500k$

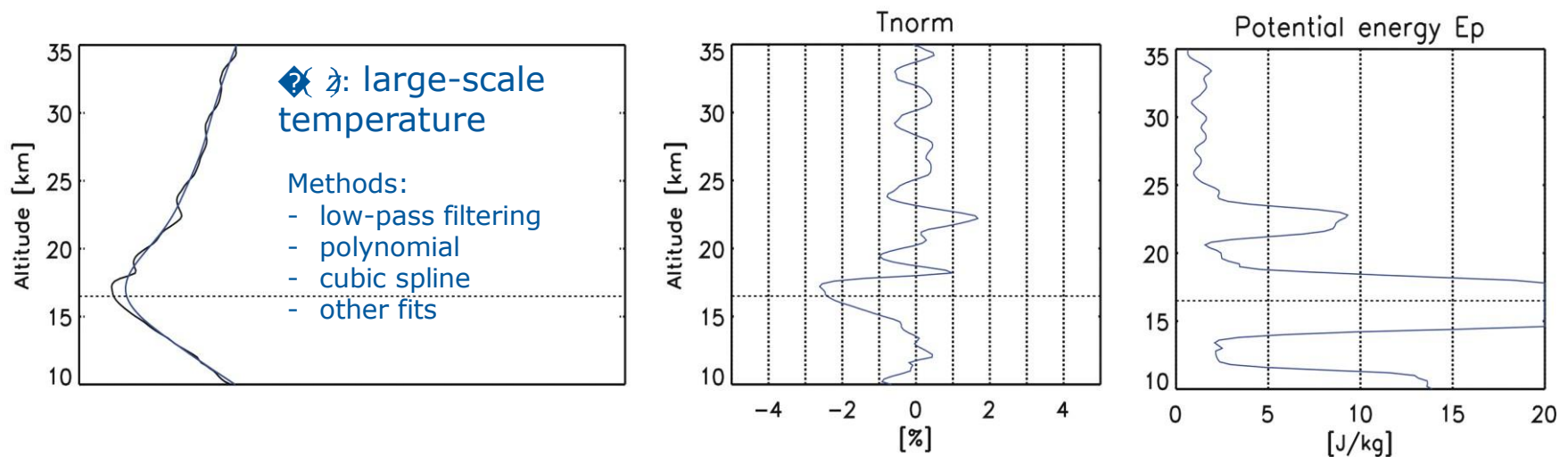
λ_h from adjacent profiles after

$$\text{Ern et al. (2004): } k_h = \frac{\Delta \phi}{\Delta x}$$

Gravity wave analysis

Background determination $\diamond(z)$
)
 $\diamond(z) \neq \diamond(z) - \diamond(z)$

Vertical detrending

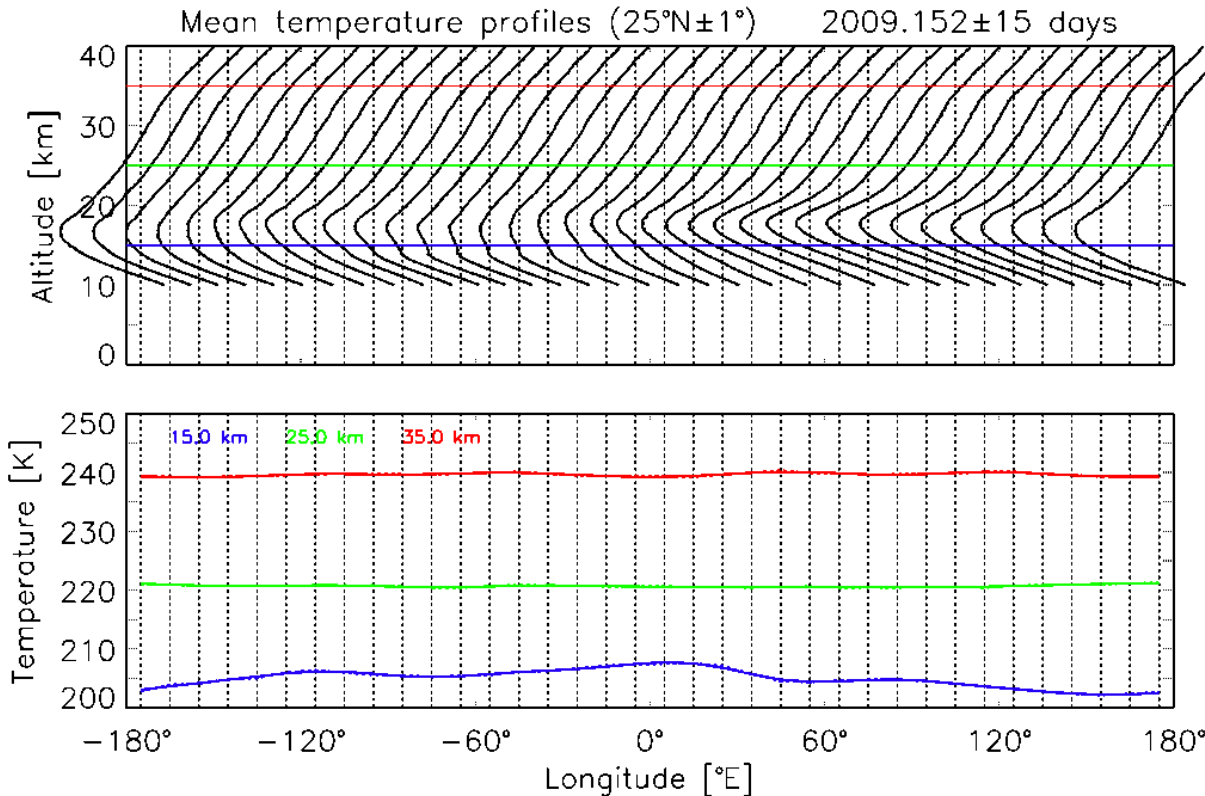


Problems especially in the tropopause region

- separate filtering (*Schmidt et al.*, GRL, 2008)
- double filtering (*P. Alexander et al.*, AMT, 2011)

Gravity wave analysis

Horizontal detrending



Temperature background (large-scale temperature)

Dynamical RO climatologies
 $\Delta t = 1$ day (10°x15° lat/lon)
 $\Delta t = \pm 3$ days (10°x15° lat/lon)
 $\Delta t = \pm 7$ days (10°x15° lat/lon)
 $\Delta t = \pm 15$ days (2°x10° lat/lon)
 (Yan et al., 2010 for HIRDLS)

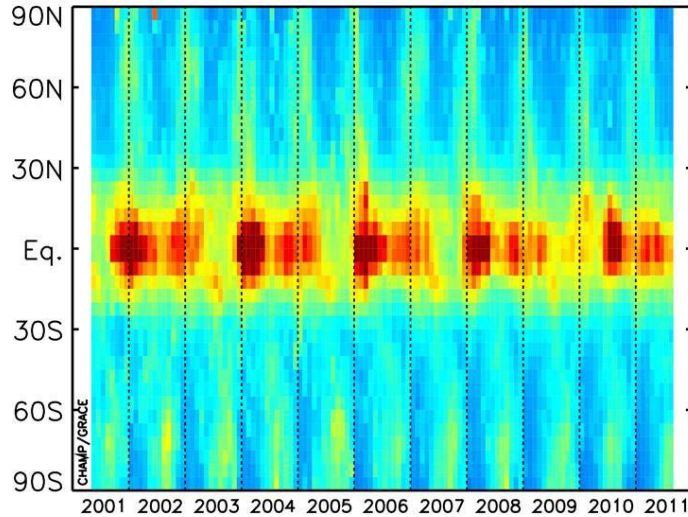
WN 1-6 from the longitudinal variations at each altitude (10-40 km, $\Delta z = 100$ m) are determined using a FFT and finally WN 0-6 define the temperature background
 (Alexander et al., 2008 for HIRDLS)

$\langle z \rangle$: large-scale (dependent on Δt) plus small-scale structures superposed

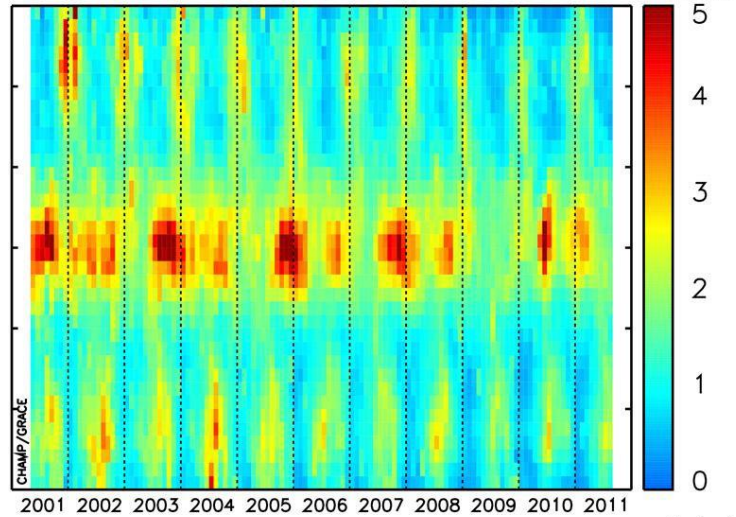
$\langle z \rangle = [\dots] - p \dots (2-15k \dots)$: isolated small-scale structures addressed to GW

Gravity wave potential energy

20–25km, $\lambda_z=2-10$ km

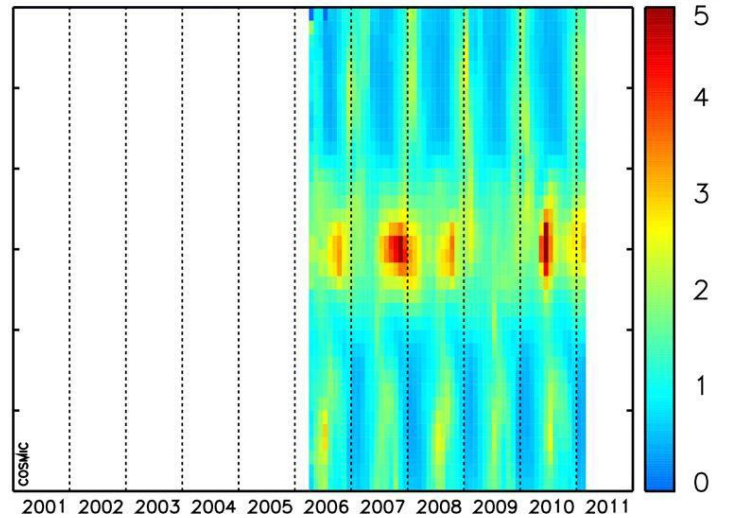
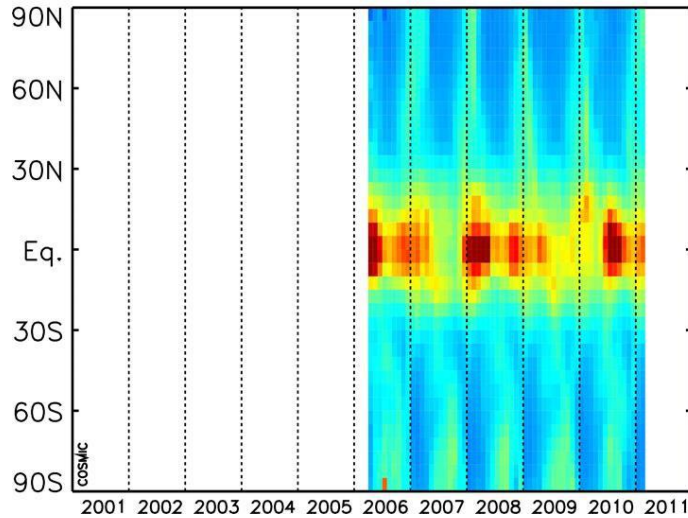


25–30km, $\lambda_z=2-10$ km



[J/kg]

GFZ
CHAMP/GRACE
May 2001-Aug 2011
 $\Delta\phi=5^\circ$
overlapping bins

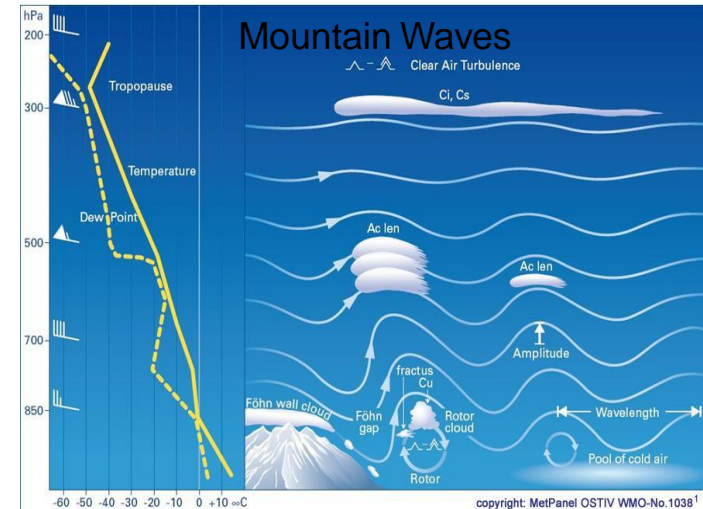
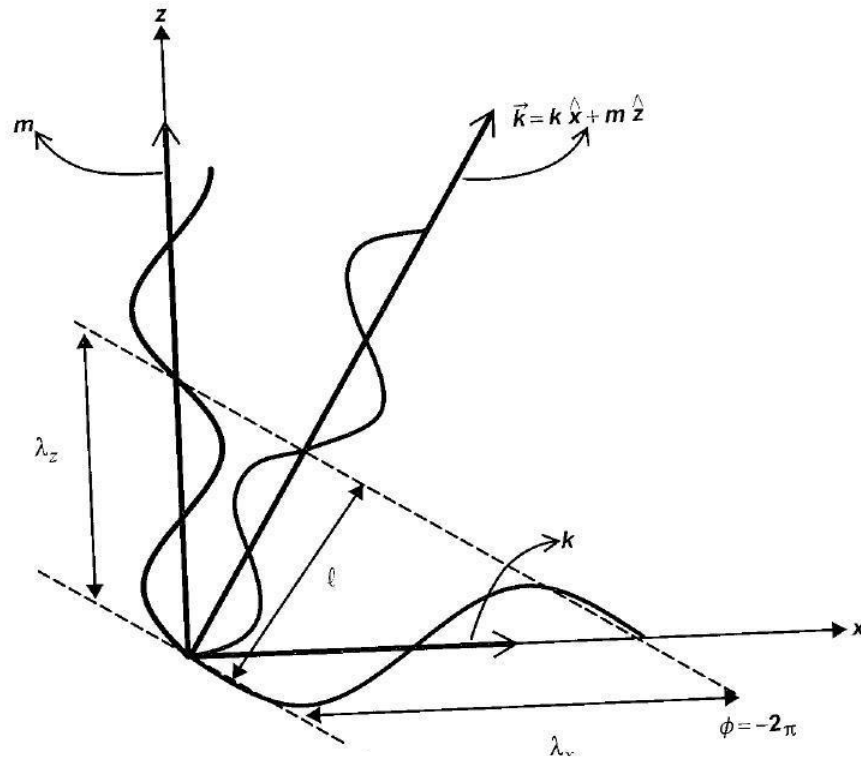


[J/kg]

UCAR
COSMIC
Apr 2006-Feb 2011
 $\Delta\phi=5^\circ$
overlapping bins

Gravity wave analysis

Determination of horizontal wave parameters



Determination of the phase shift between adjacent temperature profiles

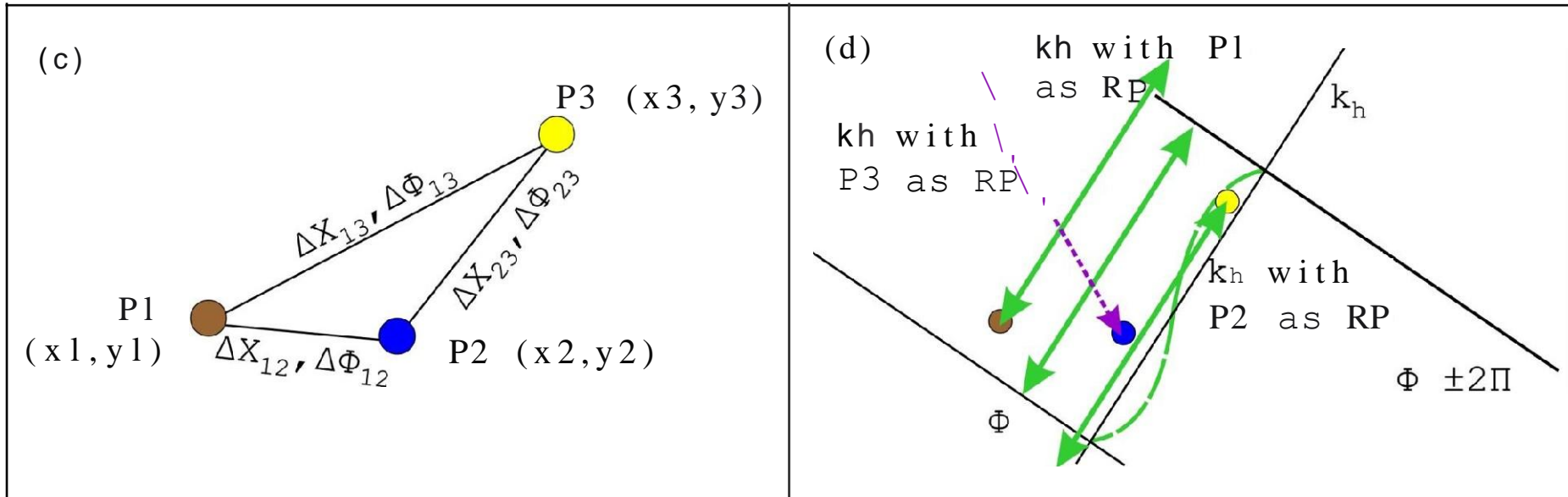
$$T'(x_h, z, t) = \bar{T}(z) \sin(\phi)$$

$$k_h = \frac{\Delta\phi_{i,j}}{\Delta x_{i,j}}$$

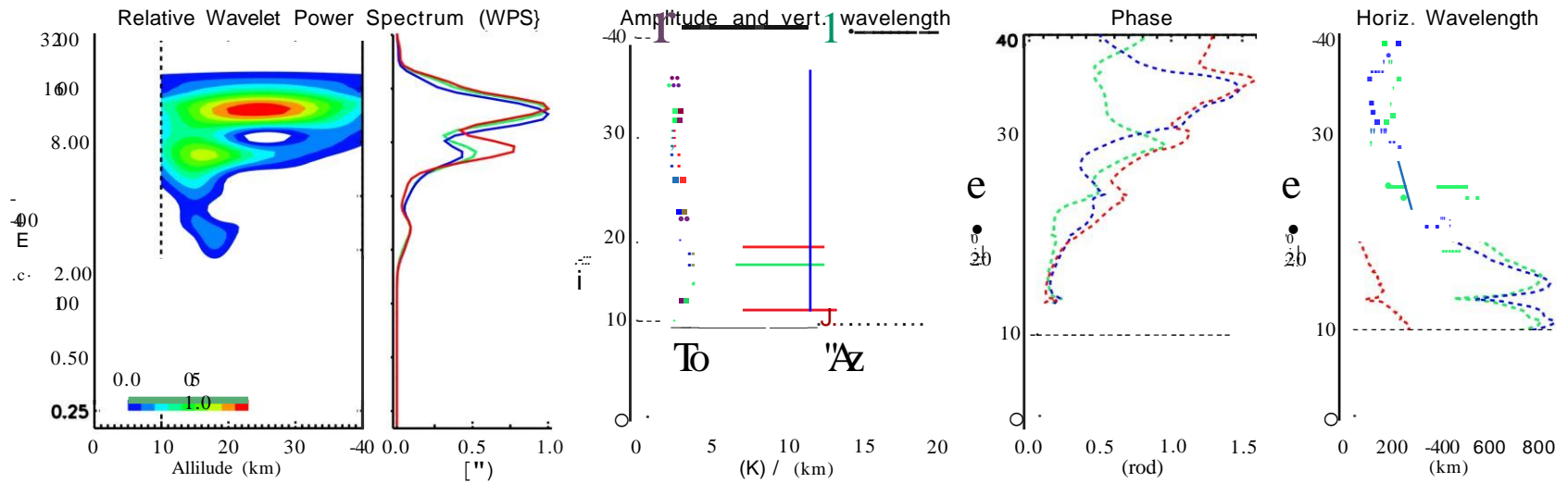
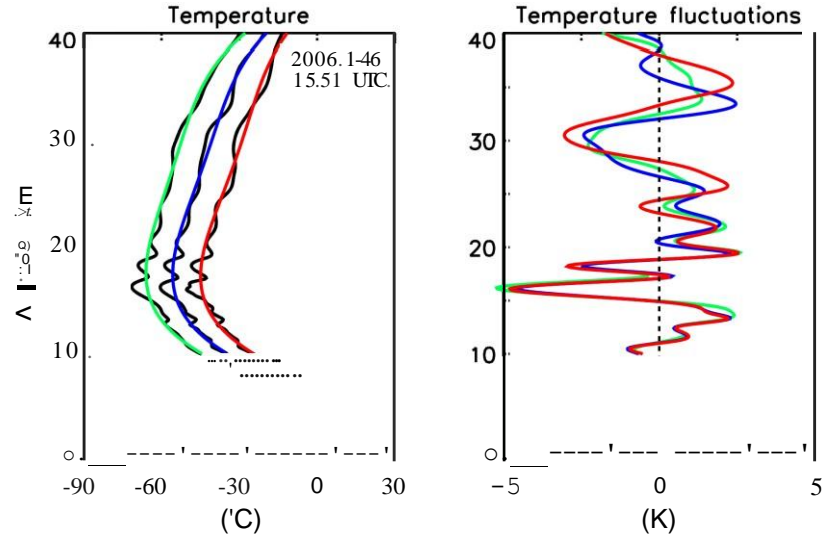
PhD work from A. Faber (GFZ) and Faber et al. (2013)

Gravity wave analysis

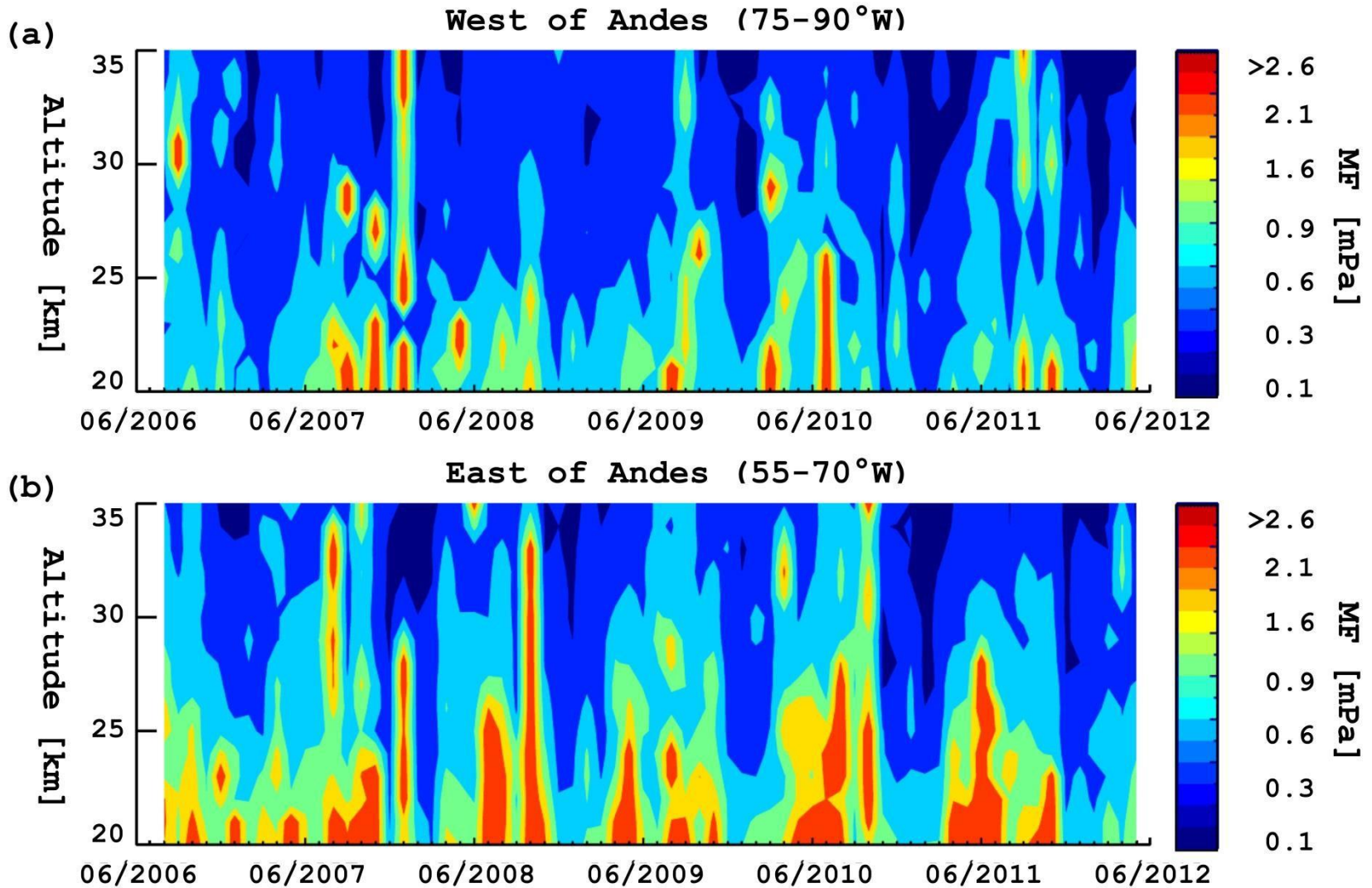
$$c_{ij} = k(x_i - x_j) + l(y_i - y_j)$$



Gravity wave analysis

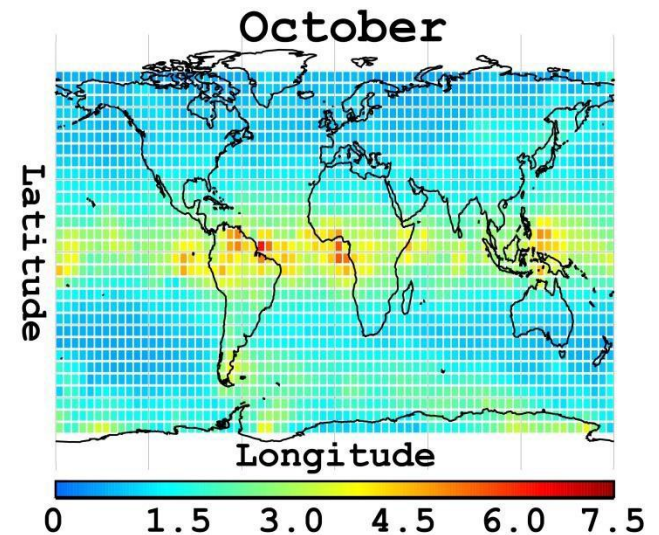
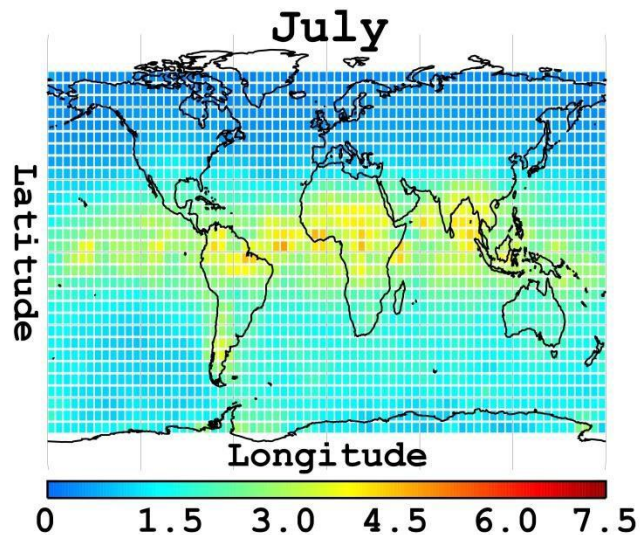
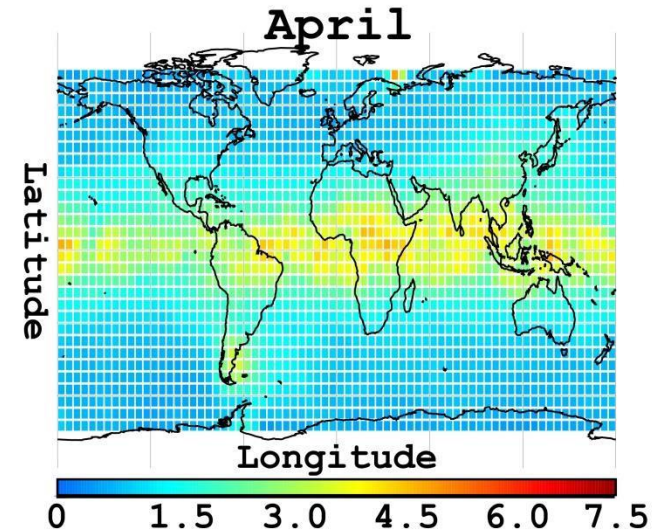
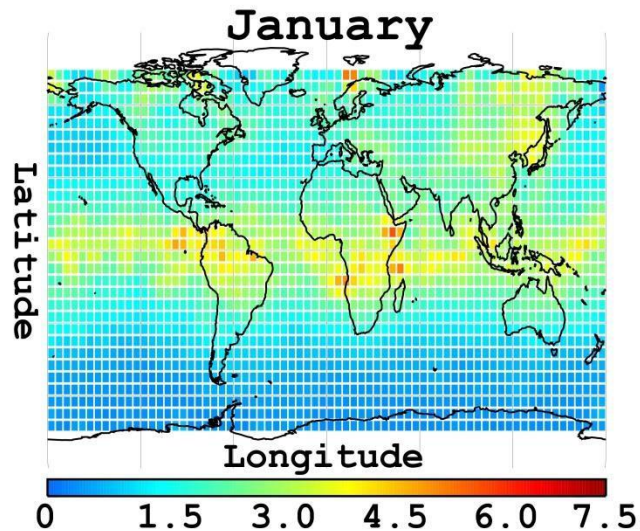


Momentum flux



Gravity wave analysis

- 4 year Monthly mean 2007-2010
- 20-25 km altitude
- Enhancement in equator region and on the local winter hemisphere
- Shift of the ITCZ is detected



(Faber et al., AMT 2013)

Summary I

GPS RO is a satellite-to-satellite limb measurement.

Outlined the basic physics of the GPS RO technique and the classical retrieval.

Measurements **do not require bias correction.**

This may be important for climate applications.

Very good vertical resolution, but poor horizontal resolution (~ 450 km average). Also, be wary of temperature retrievals above 35 km. They mainly contain a-priori information.

Information content studies suggest GPS RO should provide good temperature information in the upper troposphere and lower/mid stratosphere.

Operational assimilation of GPS RO supports this.

Summary II

More than one decade of RO data
in a climatological sense not very long, but ...

GPS RO data are on the way to establish as a climate benchmark data set (SPARC).

GPS RO data are also useful for the detection/analysis of gravity waves in the (UT)LS.

GPS RO data are also useful to study tropopause dynamics and other processes.

Some RO (data) links

GFZ: isdc.gfz-potsdam.de
or direct tschmidt@gfz-potsdam.de

UCAR: cdaac-www.cosmic.ucar.edu/cdaac

TACC: tacc.cwb.gov.tw/en

Eumetsat: www.romsaf.org
(radio occultation meteorology – satellite application facilities)